

Learning-Based Switched Reliable Control of Cyber-Physical Systems With Intermittent Communication Faults

Xin Huang and Jiuxiang Dong, *Member, IEEE*

Abstract—This study deals with reliable control problems in data-driven cyber-physical systems (CPSs) with intermittent communication faults, where the faults may be caused by bad or broken communication devices and/or cyber attackers. To solve them, a watermark-based anomaly detector is proposed, where the faults are divided to be either detectable or undetectable. Secondly, the fault's intermittent characteristic is described by the average dwell-time (ADT)-like concept, and then the reliable control issues, under the undetectable faults to the detector, are converted into stabilization issues of switched systems. Furthermore, based on the identifier-critic-structure learning algorithm, a data-driven switched controller with a prescribed-performance-based switching law is proposed, and by the ADT approach, a tolerated fault set is given. Additionally, it is shown that the presented switching laws can improve the system performance degradation in asynchronous intervals, where the degradation is caused by the fault-maker-triggered switching rule, which is unknown for CPS operators. Finally, an illustrative example validates the proposed method.

Index Terms—Adaptive dynamic programming (ADP), communication fault, cyber-physical systems (CPSs), data-driven control, reliable control.

I. INTRODUCTION

DRIVEN by networking, computing and control techniques, cyber-physical system (CPS) can greatly improve the work efficiency of existing industrial systems [1]–[5]. On account of the dependence of the CPS's operation on data transmitted via the communication devices and networks, the system/control performance of the CPS relies heavily on the quality of the transmitted data [6]. In some practical

control applications, bad or broken communication, sudden environmental disturbances, or malfunction of either software or hardware often corrupt the transmitted data. Thus, the characteristics of the communication devices may change over time, and there may be partial or complete system failure [7], which can deteriorate performance and even diverge systems in certain cases.

In addition, since communication networks are vulnerable to attacks, and such attacks compromise transmitted data, cyber attacks are also one of the main reasons behind communication faults [8]–[11]. Recently, typical cyber attacks in CPSs, such as denial-of-service (DoS) attacks [12], [13], false data injection attacks [14], [15], replay attacks [16], [17], and other attacks [18]–[20], have been reported. To defend them, some works about secure estimation and detection have been reported in [21]–[28]. In secure control aspects, [29] introduced in great detail and provided available techniques for secure control designs against cyber-physical attacks, while [30] gives a defense analysis against malicious threats on cloud control systems via a Stackelberg game. To mitigate sensor and actuator attacks, [31] presents a moving target defense control framework. Against the adversarial attacks, [32] proposes an event-triggered secure observer-based control policy. In [33], an adaptive reliable control policy was presented to stabilise the CPSs under the frequency-constrained sensor and actuator attacks. In [34] and [35], resilient control methods against frequency- and duration-constrained DoS attacks were proposed. In [36], adaptive control architectures were presented for sensor attacks in CPSs to recover system performance. In [18] and [37], which consider simultaneous sensor and actuator attacks, adaptive control policies were proposed to ensure stability of the systems. In addition, for actuator attacks, [38] presented an adaptive integral sliding-mode control strategy such that data-driven CPSs are stable with an optimal performance.

On the other hand, it is costly and difficult to attain a system's accurate model due to the complexity of industrial systems. Furthermore, for many industrial systems, data is pervasive in every aspect of industrial production, and should be fully utilized. Due to this, data-driven controls have gained much attention [39]. In the research of data-driven controls, the adaptive dynamic programming (ADP) technique (or policy iteration (PI) algorithm), as an effective approach of solving the algebraic Riccati equation (ARE), is widely applied in order to obtain a data-driven (or model-free)

Manuscript received November 27, 2019; revised February 7, 2020, February 27, 2020; accepted March 6, 2020. This work was supported in part by the National Natural Science Foundation of China (61873056, 61473068, 61273148, 61621004, 61420106016), the Fundamental Research Funds for the Central Universities in China (N170405004, N182608004), and the Research Fund of State Key Laboratory of Synthetical Automation for Process Industries in China (2013ZCX01). Recommended by Associate Editor Shun-Feng Su. (*Corresponding author: Jiuxiang Dong.*)

Citation: X. Huang and J. X. Dong, "Learning-based switched reliable control of cyber-physical systems with intermittent communication faults," *IEEE/CAA J. Autom. Sinica*, vol. 7, no. 3, pp. 711–724, May 2020.

The authors are with the College of Information Science and Engineering, Northeastern University, Shenyang 110819, and also with the State Key Laboratory of Synthetical Automation of Process Industries, Northeastern University, Shenyang 110819, and also with the Key Laboratory of Vibration and Control of Aero-Propulsion System Ministry of Education, Northeastern University, Shenyang 110819, China. (e-mail: xinhuang6558@163.com; dongjiuxiang@ise.neu.edu.cn).

Color versions of one or more of the figures in this paper are available online at <http://ieeexplore.ieee.org>.

Digital Object Identifier 10.1109/JAS.2020.1003141

controller [40]–[44]. Both [45] and [46] studied the data-driven control problems via the zero-sum game. In order to achieve a model-free optimal controller, [47] developed a data-based policy gradient ADP algorithm. Reference [48] presented an identifier-critic-based ADP structure to online solve H_∞ control problem of nonlinear continuous-time systems. Recently, [49] developed a new model-free event-triggered optimal control algorithm for continuous-time linear systems. Finally, [50] presented an event-triggered robust control policy for unknown nonlinear systems via the neural network (NN) and ADP techniques.

Based on the above discussions, it is noted that some important problems need to be further investigated for CPS security. For instance, 1) most secure control results including [18], [31]–[34], [36], and [37], are model-based; however, the exact system knowledge for the industrial systems is usually difficult to obtain in practice. 2) Optimal/robust control problems of model-free systems without adversarial environments have been well solved via ADP-based methods [40]–[50], yet the secure control issue for data-driven CPSs remains open. 3) The communication faults in [18], [36], and [37] are supposed to be on a single transmission channels; nonetheless, the multi-transmission-channel situation has been not fully studied.

Motivated by these observation, this paper, which is written from the CPS operator's viewpoint, studies reliable control problems for data-driven CPSs under communication faults, and focuses on the intermittent faults of the multi-transmission-channel situation. The main contributions of this paper are summarized as below:

1) According to the theory of the describing function, a watermark-based anomaly detector is presented, so that the faults are classified as either detectable or undetectable to the detector. It can contribute to the effective execution of the proposed learning-based switched control policy.

2) Based on the identifier-critic-structure learning algorithm, a data-driven switch controller with a prescribed-performance-based switching law is proposed, and with the aid of the average dwell-time (ADT) approach, a fault set, which the closed-loop systems can tolerate, is given.

3) The advantages of the presented method are:

i) Different from the model-based secure control results [18], [31]–[34], [36], [37], ours is data-driven;

ii) Compared with most ADP-based model-free methods [40]–[50], ours guarantees the reliability for the case of a class of intermittent communication faults;

iii) Contrary to the switched controls under the intermittent faults [51], [52], the system knowledge and switching rule are unknown for the CPS operators in this paper;

iv) Distinct from [18], [36] and [37], the presented approach focuses on the faults in multi-transmission-channel case.

The remainder of the paper is organized as follows. Section II states problem formulations. Section III presents a new data-driven control policy to tolerate a class of intermittent communication faults. Simulation results are shown in Section IV. Section V concludes this paper.

Notations: \mathbb{R}^n is the n -dimensional vector space. $\|\cdot\|$ indicates the 2-norm of vectors or induced 2-norm of matrices.

For a matrix X , X^T represents its transpose. $X \geq 0$ ($X > 0$) means that X is a symmetric positive semi-definite (positive definite) matrix with an appropriate dimension. $\text{diag}\{x_1, x_2, \dots, x_m\}$ denotes a diagonal matrix with x_1, x_2, \dots, x_m in its main diagonal. I indicates an identity matrix with a suitable dimension. \otimes means the Kronecker product. $\text{vec}(X) = [x_1^T, \dots, x_m^T]^T$, where x_i is the i th column of $X \in \mathbb{R}^{n \times m}$. For a square matrix X , $\text{He}(X) = X^T + X$. $w \in L_2(0, \infty)$ means $\int_0^\infty w^T(t)w(t)dt < \infty$.

II. PROBLEM FORMULATION

This paper considers the architecture of data-driven CPSs, as shown in Fig. 1, and the models of the physical system and communication faults are depicted as follows.

A. Physical System

The physical system can be described by the following linear time-invariant system

$$\dot{x}(t) = Ax(t) + B_u u(t) + B_d d(t) \quad (1)$$

where $x(t) \in \mathbb{R}^n$, $u(t) \in \mathbb{R}^m$ and $d(t) \in \mathbb{R}^p$ are the measurable system state, control input and external disturbance, respectively. A , B_u and B_d are all unknown matrices with appropriate dimensions. It is assumed that the pair (A, B_u) is controllable, $d \in L_2(0, \infty)$ and there is no packet dropout and delay in the transmission channels (or network layer). For the sake of simplicity, the dependence of the functions (e.g., \dot{x} , x , $u(t)$, $d(t)$, etc) on t is omitted in some cases.

Remark 1: This paper mainly focuses on reliable controls under the case of no packet dropout and delay in the transmission channel. Such an assumption was found in [18], [31]–[33], [36] and [37], and contributes to simplifying the system models such that we are only concerned with the reliable controller design under the faults. Actually, in practice, the packet dropout and delay are common in the networked control systems. They may influence the control performance. Nevertheless, [29] and [30] have developed some effective methods to solve them, thus, in future work, we will further investigate CPS reliable controls for packet-dropout and delay cases with the aid of the nice results in [29] and [30].

B. Intermittent Communication Fault

In this paper, the communication channels used to transmit sensor output signals are assumed to be vulnerable to the faults. In reality, communication faults are common in CPSs, and have been investigated in [18], [36] and [37]. Reference [36] has also reported that faults exist in some practical systems such as control systems of unmanned air vehicles. The model is usually represented by $\delta_s(x)$. In [18], [36] and [37], it is parameterized as $\delta_s(x) = \omega_s(t)x$, with the gain $\omega_s(t) \in \mathbb{R}$ subject to $\omega(t) \neq -1$. The system state compromised by the faults (i.e., that the controller receives) is given by

$$\tilde{x} = x + \delta_s(x).$$

It can be written as $\tilde{x} = \lambda(t)x$ with $\lambda(t) = 1 + \omega_s(t)$, $\lambda(t) \neq 0$ and $\|\lambda(t)\| \leq \bar{\lambda}$ (please refer to [18], [36] and [37] for the interested reader). This means the faults are on a single transmission channel. However, this paper focuses on the

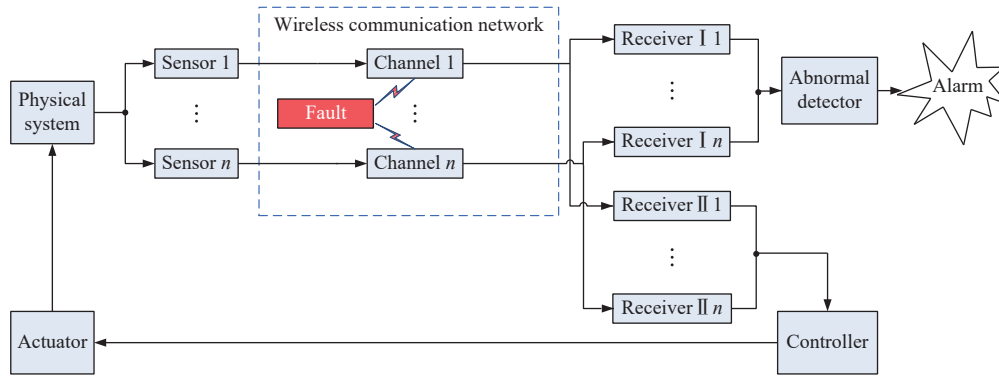


Fig. 1. Subsystem architecture of cyber-physical systems under communication faults.

multi-transmission-channel case, namely

$$\tilde{x}(t) = \Lambda x(t) \quad (2)$$

where the compromised system state $\tilde{x} = [\tilde{x}_1^T, \tilde{x}_2^T, \dots, \tilde{x}_n^T]^T$ and the parameter $\Lambda = \text{diag}\{\lambda_1, \lambda_2, \dots, \lambda_n\}$.

Additionally, as reported in [51] and [52], the fault usually has intermittent and random characteristics. Then, to describe the intermittent characteristic of fault (2), we introduce the concept of average dwell-time (ADT), which has been used to describe intermittent DoS attacks [29], [34], [35]. Inspired by definitions in [29], [34] and [35], let $\{t_i\}_{i \in \mathbb{N}}$ with $t_0 \geq 0$ denote the sequence of the fault on/off and off/on transitions. Without loss of generality, let $T_k := [t_{2k+1}, t_{2k+2})$ (for $k \in \mathbb{N}$) mean the k th time interval where the fault is active. Then, define

$$\Upsilon(\tau, t) := \bigcup_{k \in \mathbb{N}} T_k \cap [\tau, t], \quad \tilde{\Upsilon}(\tau, t) := [\tau, t] \setminus \Upsilon(\tau, t)$$

where $\Upsilon(\tau, t)$ and $\tilde{\Upsilon}(\tau, t)$ represent the subsets of $[\tau, t]$, in which there is the fault and no fault, respectively. Meanwhile, let $|\Upsilon(\tau, t)|$ and $|\tilde{\Upsilon}(\tau, t)|$ indicate the total lengths of the occurring fault and no fault within the interval $[\tau, t]$. Thus, the gain in (2) can be denoted as

$$\Lambda = \begin{cases} \Lambda \neq I, & t \in \Upsilon(0, \infty) \\ I, & t \in \tilde{\Upsilon}(0, \infty). \end{cases}$$

Let $n(\tau, t)$ represent the number of the faults occurring in the interval $[\tau, t]$. Thus, the following assumptions are given to describe the intermittent characteristic of the fault in (2).

Assumption 1 (Fault frequency [34], [35]): There exist constants $\eta_f \geq 0$ and $\tau_D > 0$ such that

$$n(\tau, t) \leq \eta_f + \frac{t - \tau}{\tau_D}.$$

Assumption 2 (Fault duration [34], [35]): There exist constants $\kappa \geq 0$, $T_1 \geq 1$ and $1 \geq 1/T_1 \geq T_2 \geq 0$ such that

$$T_2(t - \tau) \leq |\Upsilon(\tau, t)| \leq \kappa + \frac{t - \tau}{T_1}.$$

Remark 2: In our work, Assumptions 1 and 2 are similar to those in [34] and [35], and are used to constrain the fault signal in terms of its average frequency and duration. Following [34] and [35], τ_D indicates the average dwell-time between consecutive fault off/on transitions; η_f means the chattering bound; $1/T_1$ and T_2 respectively provide an upper bound and a lower bound on the average duration of the fault

per unit time; analogous to η_f , κ plays the role of a regularization term. Note that the considered fault may be always active, then T_1 in Assumption 2 satisfies $T_1 \geq 1$ not $T_1 > 1$.

The objective in this paper is to give a reliable control scheme such that the systems under the communication faults are stable.

III. RELIABLE CONTROL SCHEME OF DATA-DRIVEN CPSS WITH COMMUNICATION FAULTS

From the Laplace transform of (2), it follows that $\tilde{X}(j\omega) = \Lambda X(j\omega)$ with frequency ω . This means that the fault only damages the value of the sensor data, and does not change its frequency. According to the characteristic, a periodic oscillation with a known fixed frequency and amplitude is inserted into sensor transmission channels, and then, based on the amplitude change of the oscillation, the system checks whether it is under faults or not; meanwhile, according to the characteristic of the fixed frequency, a filter, equipped at the position of the controller side, is used to eliminate the effect of the introduced oscillation. In reality, the frequency of the introduced oscillation can be designed such that the oscillation, and, the input and output of the system (1) are in different frequency domains, thus, in such a way, a filter is used to effectively eliminate the oscillation. However, in theory, it is simple to produce a periodic oscillation. By contrast, in practice, the oscillation is very sensitive to parameter changes. Hence, according to the describing function theory [53], we can design an oscillation which is robust to disturbance, noise and uncertainty. Then, the expected oscillation is generated and injected into communication channels by the way shown in Fig. 2. In Fig. 2, we consider a smart sensor i , which performs a process measurement (i.e., sensor i to measure the system state), and a “closed-loop” to generate a desired oscillation to check whether the sensor communication channel is faulty, where $G(s)$ is the transfer function with the sufficient low-pass behavior, and $N(\mathcal{A})$ is the describing function of a nonlinear function. In “closed-loop”, $-y_2$ and v are the input and output of $N(\mathcal{A})$, respectively. y_1 is the output of $G(s)$, and r is zero-reference input of “closed-loop”. In addition, since y_1 is needed to be fed-back for “closed-loop”, a acknowledgement-based protocol is needed. It is noted that, for no fault case, $y_2 = y_1$; otherwise, $y_2 = \lambda_i y_1$. To facilitate the analysis,

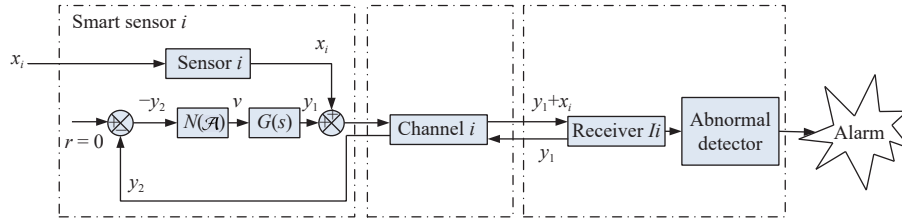


Fig. 2. A mechanism of producing a period oscillation with a fixed frequency and amplitude in i th sensor transmission channel.

suppose that the system state x and the desired oscillation y_1 are low- and high-frequency signals, respectively, and, Receiver I_i in “closed-loop” has a high-pass behavior. Thus, in this setting, after the signal $y_1 + x_i$ enters Receiver I_i , the output of the receiver approximates to the signal y_1 . For the Fourier series of the periodic signal $v(t)$ with period T , the input and output of transfer function $G(s)$ can be written as

$$v(t) = a_0 + \sum_{n=1}^{\infty} [a_n \cos(n\omega_0 t) + b_n \sin(n\omega_0 t)]$$

$$y_1(t) = G(0)a_0 + \sum_{n=1}^{\infty} |G(jn\omega_0)| [a_n \cos(n\omega_0 t) + b_n \sin(n\omega_0 t)].$$

According to the theory of the describing function [53], the describing function of the nonlinear function is denoted as

$$N(\mathcal{A}) = \frac{v(j\omega_0 t)}{e_y(j\omega_0 t)} = \frac{1}{\mathcal{A}}(b_1 + ja_1)$$

where $e_y(\cdot) = -y_2(\cdot)$, and \mathcal{A} denotes the oscillation amplitude received by the detector. From the Nyquist criterion, it is known that if the open loop transfer function $G_0(\mathcal{A}, j\omega) = N(\mathcal{A})G(j\omega)$ crosses the critical point $(-1 + j0)$, a periodic oscillation with the fixed frequency ω and amplitude \mathcal{A} will be produced, where ω and \mathcal{A} satisfy the following equalities

$$G_0(\mathcal{A}, j\omega) = N(\mathcal{A})G(j\omega) = -1$$

$$G(j\omega) = \frac{-1}{N(\mathcal{A})} = N_I(\mathcal{A}) \quad (3)$$

where $N_I(\mathcal{A})$ represents the inverse describing function, which depends on the signal amplitude \mathcal{A} . So, by designing $G(s)$ and $N(\mathcal{A})$, a period oscillation with the expected ω and \mathcal{A} can be obtained.

Without loss of generality, it is assumed that the input and output of system (1) are both low-frequency signals, and receivers of the controller and detector have the characteristics of the sufficient low- and high-pass filtering, respectively (it is worth noting that, under the assumption that the receivers of the controller have low-pass filtering, the sensor data received by the controller approximates to x). To detect abnormalities successfully, a high-frequency oscillation is generated and introduced into the sensor transmission channels. In this paper, the nonlinear function is chosen to have the ideal relay characteristic because the inverse describing function $N_I(\mathcal{A}) = -\frac{\pi\mathcal{A}}{4M}$ is a linear function about \mathcal{A} , where $M > 0$ is the maximum output of the nonlinear function. From (3), it is easily deduced that under the communication fault (2), the amplitude \mathcal{A}_1 of the oscillation received by the abnormal

detector is obtained as

$$\mathcal{A}_1 = \frac{4M|\lambda_i|}{\pi} |G(j\omega)|. \quad (4)$$

Based on (4), the detection criterion is given in the following form

$$H_0 : \underline{\mathcal{A}} \leq \mathcal{A}_1 \leq \bar{\mathcal{A}} \quad H_1 : \mathcal{A}_1 < \underline{\mathcal{A}} \text{ or } \bar{\mathcal{A}} < \mathcal{A}_1 \quad (5)$$

where \mathcal{A} is the oscillation amplitude. $\underline{\mathcal{A}} = \frac{4M\underline{\lambda}}{\pi} |G(j\omega)|$, and, $\bar{\mathcal{A}} = \frac{4M\bar{\lambda}}{\pi} |G(j\omega)|$. $\underline{\lambda}$ and $\bar{\lambda}$ are known positive constants satisfying $0 < \underline{\lambda} < 1 < \bar{\lambda}$, which are set in advance by the CPS operators. H_0 means that the system is normal operation. H_1 indicates that the system is abnormal, thus, the detector triggers an alarm. The system will then stop running to be checked.

Remark 3: The detection mechanism (5) can detect whether the i th transmission channel is under faults or not, and the faults are divided into the detectable faults satisfying $|\lambda_i| < \underline{\lambda}$ or $\bar{\lambda} < |\lambda_i|$, and relatively undetectable faults satisfying $\underline{\lambda} \leq |\lambda_i| \leq \bar{\lambda}$. By applying this detection method to all (or unreliable) channels, it is checked whether the overall sensor transmission channels are under faults, and it is restricted that parameter Λ of the communication faults is invertible.

According to the detection mechanism (5), it is known that for no-alarm cases, the communication channels might also be under faults successfully bypassing the proposed detector, thus, the reliability of the system may not be guaranteed. In the following sections, for this situation, a reliable control policy is given to stabilise the data-driven CPSs under the communication faults or no faults.

A. Switching-Based Reliable Control Strategy of CPSs Under Communication Faults

When system (1) suffers the communication fault which successfully bypasses the proposed watermark-based anomaly detector, the dynamics of the compromised system states can be depicted in the following form

$$\dot{\tilde{x}}(t) = \tilde{A}\tilde{x}(t) + \tilde{B}_u u(t) + \tilde{B}_d d(t) \quad (6)$$

where $\tilde{A} = \Lambda A \Lambda^{-1}$, $\tilde{B}_u = \Lambda B_u$, $\tilde{B}_d = \Lambda B_d$. It is known from the detector (5) that the parameter Λ is an invertible matrix. Clearly, by the fault (2), $\lim_{t \rightarrow \infty} \|\tilde{x}\| = 0$ is equivalent to $\lim_{t \rightarrow \infty} \|x\| = 0$, then the reliable control policy design of the system (1) under the faults (2) is transformed into the design of the controller to stabilise the system (6). The following lemma gives a controllability condition for (6).

Lemma 1: Considering systems (1) and (6), and the invertible matrix Λ , the pair (\tilde{A}, \tilde{B}_u) is controllable if and only if the pair (A, B_u) is controllable.

Proof: According to Theorem 9.5 in [54], it is easy to prove Lemma 1, thus, it is omitted. ■

From Lemma 1 and the controllable pair (A, B_u) , system (6) is controllable. Thus, to ensure the stability of system (6), a control policy u and a disturbance input d are given in the following forms

$$u = -K_1 \tilde{x}, \quad d = L_1 \tilde{x}.$$

The gains K_1 and L_1 of control and disturbance inputs are determined in the linear quadratic zero-sum game framework, where control and disturbance inputs are viewed as two players. It is known from the optimal theory [55] that u and d satisfy the following two-player zero-sum differential game

$$V^*(\tilde{x}(0)) = \min_u \max_d J(\tilde{x}, u, d)$$

where

$$J(\tilde{x}, u, d) = \int_0^\infty (\tilde{x}^T Q \tilde{x} + u^T R u - \gamma^2 \|d\|^2) d\tau \quad (7)$$

is the H_∞ performance index, $Q = Q^T > 0$ and $R = R^T > 0$. The pair (\tilde{A}, \sqrt{Q}) is observable and $\gamma > \gamma^*$ is the H -infinity gain. For the controllable pair (\tilde{A}, \tilde{B}_u) and accurate parameters \tilde{A} , \tilde{B}_u and \tilde{B}_d , there exists a unique $P_1^* \geq 0$ by solving the following game algebraic Riccati equation (GARE)

$$0 = P_1(\tilde{A} - \tilde{B}_u K_1 + \tilde{B}_d L_1) + (\tilde{A} - \tilde{B}_u K_1 + \tilde{B}_d L_1)^T P_1 + Q + K_1^T R K_1 - \gamma^2 L_1^T P_1. \quad (8)$$

The optimal feedback gain matrix K_1^* in (10) and L_1^* in (11) can be determined by

$$K_1^* = R^{-1} \tilde{B}_u^T P_1^*, \quad \text{and} \quad L_1^* = \frac{1}{\gamma^2} \tilde{B}_d^T P_1^*$$

and u^* and d^* satisfy the following inequalities

$$J(\tilde{x}, u^*, d) \leq J(\tilde{x}, u^*, d^*) \leq J(\tilde{x}, u, d^*).$$

On the other hand, it is noted from (6) that if $\Lambda = I$, (6) reduces to system (1); thus, in that case, the control policy u and the worst disturbance input d are designed by the above-mentioned method, and are given by

$$u = -K_0^* \tilde{x} \\ d = L_0^* \tilde{x}$$

where $\tilde{x} = x$. $K_0^* = R^{-1} B_u^T P_0^*$, $L_0^* = \frac{1}{\gamma^2} B_d^T P_0^*$, and $P_0^* \geq 0$ is a solution of (8) with A , B_u , B_d , K_0 and L_0 . From the optimal control theory, it is known that the H_∞ control pairs $u = -K_0^* x$, $d = L_0^* x$ and $u = -K_1^* \tilde{x}$, $d = L_1^* \tilde{x}$ can guarantee that the time derivatives of $\mathcal{V}_0 = x^T P_0^* x$ and $\mathcal{V}_1 = \tilde{x}^T P_1^* \tilde{x}$ are less than zero, respectively, i.e., under the H_∞ control pairs, $\dot{\mathcal{V}}_0 \leq -\alpha_0^* \mathcal{V}_0$ and $\dot{\mathcal{V}}_1 \leq -\alpha_1^* \mathcal{V}_1$, where

$$\alpha_0^* = \lambda_{\min}^{-1}(P_0^*) \lambda_{\min}(-He(P_0^* A - P_0^* B_u K_0^* + P_0^* B_d L_0^*))$$

and

$$\alpha_1^* = \lambda_{\min}^{-1}(P_1^*) \lambda_{\min}(-He(P_1^* \tilde{A} - P_1^* \tilde{B}_u K_1^* + P_1^* \tilde{B}_d L_1^*)).$$

Based on the aforementioned description and the intermittency of the communication fault (2), the reliable control problem of system (1) under fault (2) can be converted into a problem to stabilise the following virtual switched

system, which is switching between subsystems (1) and (6)

$$\dot{\tilde{x}}(t) = \bar{A}_{\sigma(t)} \tilde{x}(t) + \bar{B}_{u\sigma(t)} u_{\sigma'(t)}(t) + \bar{B}_{d\sigma(t)} d_{\sigma'(t)}(t) \quad (9)$$

where $\sigma(t) \in \{0, 1\}$ is the switched signal of the system (9), which is determined by the fault maker. $\sigma'(t) \in \{0, 1\}$ is the switched law of $u_{\sigma'(t)}$ and $d_{\sigma'(t)}$, to be determined, where

$$u_{\sigma'(t)} = -K_{\sigma'(t)} \tilde{x} \quad (10)$$

$$d_{\sigma'(t)} = L_{\sigma'(t)} \tilde{x} \quad (11)$$

where

$$\begin{cases} K_0 = K_0^*, L_0 = L_0^*, & \text{if } \sigma' = 0 \\ K_1 = K_1^*, L_1 = L_1^*, & \text{otherwise.} \end{cases}$$

$\sigma(t) = 0$ indicates that subsystem (1) is active, i.e., the system is under normal operation, otherwise, $\sigma(t) = 1$ means that the subsystem (6) is active. The corresponding system parameters are given in the following:

$$\begin{cases} \bar{A}_0 = A, \bar{B}_{u0} = B_u, \bar{B}_{d0} = B_d, & \text{if } \sigma = 0 \\ \bar{A}_1 = \tilde{A}, \bar{B}_{u1} = \tilde{B}_u, \bar{B}_{d1} = \tilde{B}_d, & \text{otherwise.} \end{cases}$$

The fault maker may be a smarter attacker and their aims may be to degrade the system/control performance as much as possible. On account of their intelligence, the fault-maker-triggered switching law $\sigma(t)$ is generally unknown for the CPS operators. So, it is a challenging problem to give a suitable switching law $\sigma'(t)$ of the controller such that the system (9) is stable. Fig. 3 describes the relationship of $\sigma(t)$ and $\sigma'(t)$. Without loss of generality, it is assumed that $t'_{2k+1} \neq t_{2k+1}$ for any k . By Fig. 3, there always exists an interval $[t'_{2k+1}, t_{2k+1})$ or $[t_{2k+1}, t'_{2k+1})$ caused by the wrong switching, in which the system may be unstable. To address this problem, a new switching law based on a prescribed performance function is proposed in this paper, and it is given in the following form:

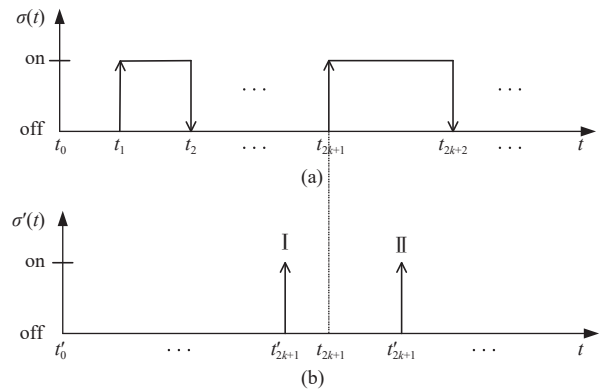


Fig. 3. Relationship between $\sigma(t)$ and $\sigma'(t)$. on/off transitions are represented as \downarrow , while off/on transitions are represented as \uparrow . For $k = 0, 1, \dots$, (a) off/on transitions occurring at t_{2k+1} indicate that the faults occur and on/off transitions occurring at t_{2k+2} mean that the faults stop; (b) off/on transitions occurring at t'_{2k+1} indicate that the mode 0 of the controller switches the mode 1 (i.e., the CPS operator thinks that the faults occur), and on/off transitions occurring at t'_{2k+2} mean that the mode 1 of the controller switches the mode 0 (i.e., the CPS operator thinks that the faults stop).

$$\sigma'(t) = \begin{cases} i, & \mathcal{V}_i^*(t) \leq \epsilon_i(\mathcal{V}_i^*(t'_k)) \\ 1-i, & \mathcal{V}_i^*(t) > \epsilon_i(\mathcal{V}_i^*(t'_k)) \end{cases} \quad (12)$$

where $i \in \{0, 1\}$. $\sigma'(t^-) = i$, and $t^- < t$. ϵ_i means the prescribed performance function, and is described by

$$\epsilon_i(\mathcal{V}_i^*(t'_k)) = \eta_0 e^{-a_i^*(t-t'_k)} \mathcal{V}_i^*(t'_k) + \eta_\infty$$

where η_0, η_∞ are positive constants and satisfy $\eta_0 \geq 1, \eta_\infty \geq 0$. $\mathcal{V}_i^* = \bar{x}^T P_i^* \bar{x}$. $a_i^* > 0$ satisfies $a_i^* < \alpha_i^*$ where α_i^* is a known constant, and $\alpha_i^* = \lambda_{\min}^{-1}(P_i^*) \lambda_{\min}(-\text{He}(P_i^* \bar{A}_i - P_i^* \bar{B}_{ui} K_i^* + P_i^* \bar{B}_{di} L_i^*))$ for $i \in \{0, 1\}$.

Lemma 2: Denote the time sequence consisted of the no fault time interval $[t_{2i}, t_{2i+1})$ and fault-activated time interval $[t_{2i+1}, t_{2i+2})$, $i = 0, 1, \dots, k$, as $\iota = (t_0, t_1, \dots, t_{2k+1}, t_{2k+2})$ and the switching time sequence generated by the switched law (12) under the sequence ι as $\iota' = (t'_0, t'_1, \dots, t'_{2k+1}, t'_{2k+2})$, thus, the following inequalities are satisfied

$$\begin{aligned} t'_{2k+1} - t_{2k+1} &\leq \left(\frac{1}{a_i^*} + \frac{1}{\alpha_i^* - a_i^*} \right) \ln(\eta_0) \\ &+ \left(\frac{1}{a_i^*} + \frac{1}{\alpha_i^* - a_i^*} \right) \ln(\bar{\mu}_i(t'_{2k+1}, t'_{2k})) + \ln\left(\frac{\mathcal{V}_{\sigma'(t)}^*(t'_{2k})}{\mathcal{V}_{\sigma'(t)}^*(t'_{2k+1})} \right) \end{aligned}$$

and

$$\begin{aligned} t'_{2k+2} - t_{2k+2} &\leq \left(\frac{1}{a_{1-i}^*} + \frac{1}{\alpha_{1-i}^* - a_{1-i}^*} \right) \ln(\eta_0) \\ &+ \left(\frac{1}{a_{1-i}^*} + \frac{1}{\alpha_{1-i}^* - a_{1-i}^*} \right) \ln(\bar{\mu}_{1-i}(t'_{2k+2}, t'_{2k+1})) \\ &+ \ln\left(\frac{\mathcal{V}_{\sigma'(t)}^*(t'_{2k+1})}{\mathcal{V}_{\sigma'(t)}^*(t'_{2k+2})} \right) \end{aligned}$$

where

$$\begin{aligned} \bar{\mu}_i(\bar{t}_1, \bar{t}_2) &= 1 + e^{\frac{\ln(\frac{\eta_\infty}{\mathcal{V}_{\sigma'(t)}^*(\bar{t}_2)}) - \ln(\eta_0) + a_i^*(\bar{t}_1 - \bar{t}_2)}{\alpha_i^* - a_i^*}} \\ \mathcal{V}_{\sigma'(t)}^*(t'_{2k+1}) &= \eta_0 e^{-a_i^*(t'_{2k+1} - t'_{2k})} \mathcal{V}_{\sigma'(t)}^*(t'_{2k}) + \eta_\infty \\ \mathcal{V}_{\sigma'(t)}^*(t'_{2k+2}) &= \eta_0 e^{-a_{1-i}^*(t'_{2k+2} - t'_{2k+1})} \mathcal{V}_{\sigma'(t)}^*(t'_{2k+1}) + \eta_\infty \end{aligned}$$

and

$$\dot{\mathcal{V}}_{\sigma'(t)}^* = \bar{x}^T P_{\sigma'(t)}^* \bar{x} \quad (13)$$

where $\sigma'(t) = i$ for $t \in [t'_{2k}, t'_{2k+1})$ and $i \in \{0, 1\}$.

Proof: From the switching law (12), it is known that the time interval $[t_{2k+1}, t'_{2k+1})$ or $[t_{2k+2}, t'_{2k+2})$ is caused by the delay switching. Without loss of generality, we consider the time interval $[t'_{2k}, t_{2k+1}) \cup [t_{2k+1}, t'_{2k+1})$, in which the mode $\sigma'(t)$ of the controller is i , thus, for $t \in [t'_{2k}, t_{2k+1})$, the time derivatives of $\mathcal{V}_{\sigma'(t)}^*$ are given by

$$\dot{\mathcal{V}}_{\sigma'(t)}^*(t) \leq -\alpha_i^* \mathcal{V}_{\sigma'(t)}^*(t)$$

which implies that

$$\mathcal{V}_{\sigma'(t)}^*(t) \leq e^{-\alpha_i^*(t-t'_{2k})} \mathcal{V}_{\sigma'(t)}^*(t'_{2k}).$$

On the other hand, from the switched law (12), for $t = t'_{2k+1}$, we have

$$\begin{aligned} \mathcal{V}_{\sigma'(t)}^*(t'_{2k+1}) &= \eta_0 e^{-a_i^*(t'_{2k+1} - t'_{2k})} \mathcal{V}_{\sigma'(t)}^*(t'_{2k}) + \eta_\infty \\ &= \eta_0 e^{-a_i^*(t'_{2k+1} - t'_{2k})} \mathcal{V}_{\sigma'(t)}^*(t'_{2k}) \\ &\quad \times (1 + \eta_\infty \eta_0^{-1} e^{a_i^*(t'_{2k+1} - t'_{2k})} (\mathcal{V}_{\sigma'(t)}^*(t'_{2k}))^{-1}) \\ &= e^{\ln(\eta_0) - a_i^*(t'_{2k+1} - t'_{2k}) + \ln(\mathcal{V}_{\sigma'(t)}^*(t'_{2k}))} e^{\ln(\bar{\mu}_i(t'_{2k+1}, t'_{2k}))} \end{aligned}$$

and, it is manipulated into

$$\begin{aligned} \ln(\mathcal{V}_{\sigma'(t)}^*(t'_{2k+1})) &= \ln(\eta_0) + \ln(\bar{\mu}_i(t'_{2k+1}, t'_{2k})) \\ &\quad + \ln(\mathcal{V}_{\sigma'(t)}^*(t'_{2k})) - a_i^*(t'_{2k+1} - t'_{2k}). \end{aligned}$$

Furthermore, the above equation can be written as

$$\begin{aligned} t'_{2k+1} - t'_{2k} &+ \frac{1}{a_i^*} (\ln(\eta_0) + \ln(\bar{\mu}_i(t'_{2k+1}, t'_{2k})) \\ &+ \ln(\frac{\mathcal{V}_{\sigma'(t)}^*(t'_{2k})}{\mathcal{V}_{\sigma'(t)}^*(t'_{2k+1})})). \end{aligned} \quad (14)$$

In addition, for $t = t_{2k+1}$, one has

$$\begin{aligned} \mathcal{V}_{\sigma'(t)}^*(t_{2k+1}) &\leq e^{-\alpha_i^*(t_{2k+1} - t'_{2k})} \mathcal{V}_{\sigma'(t)}^*(t'_{2k}) \\ &\leq \eta_0 e^{-a_i^*(t_{2k+1} - t'_{2k})} \mathcal{V}_{\sigma'(t)}^*(t'_{2k}) + \eta_\infty \end{aligned}$$

the above inequality can be manipulated into

$$\begin{aligned} -\alpha_i^*(t_{2k+1} - t'_{2k}) + \ln(\mathcal{V}_{\sigma'(t)}^*(t'_{2k})) &\leq \ln(\eta_0) \\ &+ \ln(\bar{\mu}_i(t_{2k+1}, t'_{2k})) + \ln(\mathcal{V}_{\sigma'(t)}^*(t'_{2k})) - a_i^*(t_{2k+1} - t'_{2k}) \end{aligned}$$

thus, by some mathematical operations, we have

$$\begin{aligned} -(t_{2k+1} - t'_{2k}) &\leq \frac{1}{\alpha_i^* - a_i^*} (\ln(\eta_0) + \ln(\bar{\mu}_i(t_{2k+1}, t'_{2k}))) \\ &\leq \frac{1}{\alpha_i^* - a_i^*} (\ln(\eta_0) + \ln(\bar{\mu}_i(t'_{2k+1}, t'_{2k}))). \end{aligned} \quad (15)$$

Based on (14) and (15), we have

$$\begin{aligned} t'_{2k+1} - t_{2k+1} &= -(t_{2k+1} - t'_{2k}) \\ &+ \frac{1}{a_i^*} (\ln(\eta_0) + \ln(\bar{\mu}_i(t'_{2k+1}, t'_{2k})) + \ln(\frac{\mathcal{V}_{\sigma'(t)}^*(t'_{2k})}{\mathcal{V}_{\sigma'(t)}^*(t'_{2k+1})})) \\ &\leq \left(\frac{1}{a_i^*} + \frac{1}{\alpha_i^* - a_i^*} \right) \ln(\eta_0) + \frac{1}{\alpha_i^* - a_i^*} \ln(\bar{\mu}_i(t'_{2k+1}, t'_{2k})) \\ &\quad + \frac{1}{a_i^*} \ln(\bar{\mu}_i(t'_{2k+1}, t'_{2k})) + \ln(\frac{\mathcal{V}_{\sigma'(t)}^*(t'_{2k})}{\mathcal{V}_{\sigma'(t)}^*(t'_{2k+1})}). \end{aligned}$$

For the interval $[t'_{2k+1}, t_{2k+2}) \cup [t_{2k+2}, t'_{2k+2})$, in which the mode of the controller is $1-i$, repeat the above process. Then, we obtain

$$\begin{aligned} t'_{2k+2} - t_{2k+2} &\leq \left(\frac{1}{a_{1-i}^*} + \frac{1}{\alpha_{1-i}^* - a_{1-i}^*} \right) \ln(\eta_0) \\ &+ \left(\frac{1}{a_{1-i}^*} + \frac{1}{\alpha_{1-i}^* - a_{1-i}^*} \right) \ln(\bar{\mu}_{1-i}(t'_{2k+2}, t'_{2k+1})) \\ &+ \ln(\frac{\mathcal{V}_{\sigma'(t)}^*(t'_{2k+1})}{\mathcal{V}_{\sigma'(t)}^*(t'_{2k+2})}) \end{aligned}$$

Remark 4: Note that, in the time intervals $[t_{2k+1}, t'_{2k+1})$ and $[t_{2k+2}, t'_{2k+2})$, the time derivative of the Lyapunov function (13) is greater than zero; thus, decreasing the intervals can improve the system performance. From Lemma 2, it follows

that under the switched law proposed in this paper, $t'_{2k+1} - t_{2k+1} \leq T_{\tau,2k+1}$ and $t'_{2k+2} - t_{2k+2} \leq T_{\tau,2k+2}$ can be guaranteed, and $T_{\tau,2k+1}$ and $T_{\tau,2k+2}$ are reduced by decreasing η_0 and η_∞ .

In the sequel, a main result can be depicted as follows.

Theorem 1: Consider system (9) with communication faults (2) satisfying Assumptions 1 and 2 with arbitrary η_f and κ . Denote $P_{\sigma'}^* = P_{\sigma'}^{*T} > 0$ as the solution of GARE with the mode $\sigma'(t) \in \{0, 1\}$, then,

1) for no controller-switched case, H_∞ control pair (10) and (11) with the switching law (12) guarantees $\lim_{t \rightarrow \infty} \|\bar{x}\| \leq \varepsilon$, where $\varepsilon = \eta_\infty^{-\frac{1}{2}} \lambda_{\min}^{-\frac{1}{2}}(P_{\sigma'}^*)$;

2) for the controller-switched case, if the following conditions are satisfied

$$\begin{aligned} \alpha_0^* \left(1 - \frac{1}{T_1}\right) + \alpha_1^* T_2 &> \lambda^*, \quad \lambda^* > \frac{T_\mu}{\tau_D} \\ P_0^* &< \mu P_1^*, \quad P_1^* < \mu P_0^* \end{aligned} \quad (16)$$

where $T_\mu = 2\ln(\mu) + (\beta_i^* + \alpha_{1-i}^*)T_{\tau,Mi} + (\beta_{1-i}^* + \alpha_i^*)T_{\tau,M(1-i)}$, $\beta_i^* = \lambda_{\min}^{-1}(P_i^*)\lambda_{\max}(He(P_i^* \bar{A}_{1-i} - P_i^* \bar{B}_{u(1-i)} K_i^* + P_i^* \bar{B}_{d(1-i)} L_i^*))$, $i \in \{0, 1\}$, thus, H_∞ control pair (10) and (11) with the switching law (12) guarantees that the system (9) is global asymptotically stable.

Proof: Consider the following Lyapunov function candidate

$$\mathcal{V}_{\sigma'(t)}^* = \bar{x}(t)^T P_{\sigma'(t)}^* \bar{x}(t). \quad (17)$$

The proof starts from two cases: one is where there are no switching controller, and the other is the case of switching controller for $t \in [0, \infty]$.

Case 1 (No controller-switched case): In this situation, it is assumed that the mode of the controller is i , i.e., $\sigma'(t) = i$. From the switched law (9), it is known that

$$\lambda_{\min}(P_i^*) \|\bar{x}\|^2 \leq \eta_0 e^{-\alpha_i^*(t-t'_{2k})} \mathcal{V}_i^*(t'_{2k}) + \eta_\infty$$

which implies that $\lim_{t \rightarrow \infty} \|\bar{x}\| \leq \eta_\infty^{-\frac{1}{2}} \lambda_{\min}^{-\frac{1}{2}}(P_i^*)$.

Case 2 (Controller-switched case): We consider $t \in [t'_{2k}, t_{2k+1}) \cup [t_{2k+1}, t'_{2k+1})$, in which the mode of the controller is assumed to be i , i.e., $\sigma'(t) = i$, and, in this case, there exists the interval $[t_{2k+1}, t'_{2k+1})$ in which the time derivative of the Lyapunov function is greater than zero, so, it is assumed that $\beta_i^* \geq 0$. For $t \in [t_{2k+1}, t'_{2k+1})$, the time derivative of (17) is

$$\begin{aligned} \dot{\mathcal{V}}_i^*(t) &\leq \lambda_{\max}(He(P_i^* \bar{A}_{1-i} - P_i^* \bar{B}_{u(1-i)} K_i^* \\ &\quad + P_i^* \bar{B}_{d(1-i)} L_i^*)) \|\bar{x}\|^2 \leq \beta_i^* \mathcal{V}_i^*(t) \end{aligned}$$

further, one has

$$\begin{aligned} \mathcal{V}_i^*(t) &\leq e^{\beta_i^*(t-t_{2k+1})} e^{-\alpha_i^*(t_{2k+1}-t'_{2k})} \mathcal{V}_i^*(t'_{2k}) \\ &\leq \mu e^{\beta_i^*(t-t_{2k+1}) + \beta_{1-i}^*(t'_{2k}-t_{2k})} \\ &\quad \times e^{-\alpha_i^*(t_{2k+1}-t'_{2k}) - \alpha_{1-i}^*(t_{2k}-t'_{2k-1})} \mathcal{V}_{1-i}^*(t'_{2k-1}) \\ &\leq \mu^2 e^{\beta_i^*(t-t_{2k+1}) + \beta_{1-i}^*(t'_{2k}-t_{2k}) + \beta_i^*(t'_{2k-1}-t_{2k-1})} \\ &\quad \times e^{-\alpha_i^*(t_{2k+1}-t'_{2k}) - \alpha_{1-i}^*(t_{2k}-t'_{2k-1}) - \alpha_i^*(t_{2k-1}-t'_{2k-2})} \mathcal{V}_i^*(t'_{2k-2}) \\ &= \mu^2 e^{\beta_i^*(t-t_{2k+1})} e^{(\beta_{1-i}^* + \alpha_i^*)(t'_{2k}-t_{2k})} \\ &\quad \times e^{(\beta_i^* + \alpha_{1-i}^*)(t'_{2k-1}-t_{2k-1})} e^{\alpha_i^*(t'_{2k-2}-t_{2k-2})} \\ &\quad \times e^{-\alpha_i^*(t_{2k+1}-t_{2k}) - \alpha_{1-i}^*(t_{2k}-t_{2k-1}) - \alpha_i^*(t_{2k-1}-t_{2k-2})} \mathcal{V}_i^*(t'_{2k-2}). \end{aligned}$$

From Lemma 2, it is known that $t'_{2k+1} - t_{2k+1} \leq T_{\tau,Mi}$ and $t'_{2k} - t_{2k} \leq T_{\tau,M(1-i)}$ for $k = 0, 1, \dots$, where

$$T_{\tau,Mi} \geq 0 := \max\{T_{\tau,2k+1}\}_{k=0}^\infty$$

and $T_{\tau,M(1-i)} \geq 0 := \max\{T_{\tau,2k+2}\}_{k=0}^\infty$, thus, let $t'_0 = 0$ (in fact, for t'_0 being any positive constant, just replace 0 with the corresponding t'_0 , and the following proof still holds), we have

$$\begin{aligned} \mathcal{V}_i^*(t) &\leq \mu^2 e^{\beta_i^* T_{\tau,Mi} + \alpha_i^* T_{\tau,M(1-i)}} \\ &\quad \times e^{(\beta_{1-i}^* + \alpha_i^*) T_{\tau,M(1-i)} + (\beta_i^* + \alpha_{1-i}^*) T_{\tau,Mi}} \\ &\quad \times e^{-\alpha_i^*(t_{2k+1}-t_{2k}) - \alpha_{1-i}^*(t_{2k}-t_{2k-1}) - \alpha_i^*(t_{2k-1}-t_{2k-2})} \\ &\quad \times \mathcal{V}_i^*(t'_{2k-2}) \\ &\leq \mu^{2n(0,t)} e^{\beta_i^* T_{\tau,Mi} + \alpha_i^* T_{\tau,M(1-i)}} \\ &\quad \times e^{n(0,t)((\beta_{1-i}^* + \alpha_i^*) T_{\tau,M(1-i)} + (\beta_i^* + \alpha_{1-i}^*) T_{\tau,Mi})} \\ &\quad \times e^{-\alpha_0^* |\bar{\Upsilon}(0,t)| - \alpha_1^* |\bar{\Upsilon}(0,t)|} \mathcal{V}_i^*(0) \end{aligned}$$

where $|\bar{\Upsilon}(0,t)|$ means the time of no fault in $[0, t]$, and satisfies $|\bar{\Upsilon}(0,t)| \cup |\bar{\Upsilon}(0,t)| = t$, which implies $|\bar{\Upsilon}(0,t)| \geq -\kappa + (1-1/T_1)t$. According to Assumptions 1 and 2, one has

$$\mathcal{V}_i^*(t) \leq \mu_\alpha e^{t\left(\frac{T_\mu}{\tau_D} - \lambda^* + \alpha^* - \alpha_0^* \left(1 - \frac{1}{T_1}\right) - \alpha_1^* T_2\right)} \mathcal{V}_i^*(0)$$

where $\mu_\alpha = e^{\beta_i^* T_{\tau,Mi} + \alpha_i^* T_{\tau,M(1-i)} + \eta_f T_\mu + \alpha_0^* \kappa}$, $T_\mu = 2\ln(\mu) + (\beta_{1-i}^* + \alpha_i^*) T_{\tau,M(1-i)} + (\beta_i^* + \alpha_{1-i}^*) T_{\tau,Mi}$. According to (16), it is known that

$$\delta_T = \frac{T_\mu}{\tau_D} - \alpha_0^* (1 - 1/T_1) - \alpha_1^* T_2 < 0$$

thus, one gets

$$\mathcal{V}_i^*(t) \leq \mu_\alpha e^{\delta_T t} \mathcal{V}_i^*(0)$$

which implies that system (9) is global asymptotically stable. ■

Remark 5: Note that $\lim_{t \rightarrow \infty} \|\bar{x}\| = 0$ is equivalent to $\lim_{t \rightarrow \infty} \|x\| = 0$, and it is known from Theorem 1 that the proposed control policy can ensure that the virtual switched system (9) is stable, which implies that the system states in CPSs with the controller (10) under the intermittent communication faults (2) are stable. On the other hand, parameters τ_D , T_1 and T_2 help to depict the fault frequency and duration; hence, condition (16) also means a fault set that can be tolerated by controller (10).

Theorem 1 indicates that the H_∞ control pair (10) and (11) can ensure the stability of (9), where the accurate parameters \bar{A}_σ , $\bar{B}_{u\sigma}$, $\bar{B}_{d\sigma}$ and $P_{\sigma'}^*$ need to be used in (10) and (11). However, for the data-driven CPSs, the system parameters are usually unknown. In the next section, an identifier-critic learning algorithm is used to obtain the available parameters. Then, the above-mentioned result is extended to the data-driven case.

B. Learning-Based Switched Reliable Control Policy of Data-Driven CPSs

In this section, we first assume that the unknown parameters (in (10) and (11)) for the systems under the considered faults and no faults can be estimated. Then, (6) can be written as

$$\dot{\tilde{x}} = W_1^T \psi_1(\tilde{x}, u, d) \quad (18)$$

where $W_1 = [\tilde{A} \quad \tilde{B}_u \quad \tilde{B}_d]^T$ and $\psi_1(\tilde{x}, u, d) = [\tilde{x}^T \quad u^T \quad d^T]^T$. In this

paper, the filtered variables x_f and Ψ_{1f} in [56] are introduced to identify the system parameters, and the corresponding filters are denoted as $\varsigma \dot{x}_f + x_f = \tilde{x}$, and, $\varsigma \dot{\psi}_{1f} + \psi_{1f} = \psi_1$, where $x_f(0) = 0$ and $\psi_{1f}(0) = 0$. $\varsigma > 0$ is the “bandwidth” of the filter $(\cdot)_f = (\cdot)/(\varsigma s + 1)$, and should be set small to retain robustness [48]. x_f and ψ_{1f} are obtained by applying a stable filter operation $(\cdot)_f = (\cdot)/(\varsigma s + 1)$ on \tilde{x} and ψ_1 . By this filter operation, (18) can be written as

$$\dot{x}_f = \frac{\tilde{x} - x_f}{\varsigma} = W_1^T \psi_{1f}. \quad (19)$$

Furthermore, the following auxiliary matrices $\mathcal{P}_1 \in \mathbb{R}^{(n+m+p) \times (n+m+p)}$ and $\mathcal{Q}_1 \in \mathbb{R}^{(n+m+p) \times n}$ are defined as

$$\dot{\mathcal{P}}_1 = -l_1 \mathcal{P}_1 + \psi_{1f} \psi_{1f}^T \quad (20)$$

$$\dot{\mathcal{Q}}_1 = -l_1 \mathcal{Q}_1 + \psi_{1f} \frac{(\tilde{x} - x_f)^T}{\varsigma} \quad (21)$$

where $\mathcal{P}_1(0) = 0$ and $\mathcal{Q}_1(0) = 0$. $l_1 > 0$ is a forgetting factor, and should be chosen to trade off the convergence speed and the robustness [48]. In light of (19)–(21), one gets

$$\dot{\mathcal{Q}}_1 = \mathcal{P}_1 W_1.$$

Let \hat{W}_1 and \tilde{W}_1 be the estimate and estimation error of W_1 , i.e., $\tilde{W}_1 = W_1 - \hat{W}_1$, then, the weight updating law is given by

$$\dot{\hat{W}}_1 = -\Gamma_1 (\mathcal{P}_1 \hat{W}_1 - \mathcal{Q}_1) \quad (22)$$

where $\Gamma_1 > 0$ is a learning gain matrix.

Lemma 3: Consider system (6). Under the adaptive law (22), the estimation error \tilde{W}_1 converges to zero exponentially if ψ_1 is persistently exciting (PE).

Proof: Similar to the proof of Theorem 2 in [56], thus, the corresponding proof is omitted. ■

Based on Lemma 3, system (6) can be written in the following form

$$\dot{\tilde{x}} = \hat{A}\tilde{x} + \hat{B}_u u + \hat{B}_d d + e_1 \quad (23)$$

where \hat{A} , \hat{B}_u and \hat{B}_d are the estimations of \tilde{A} , \tilde{B}_u and \tilde{B}_d , respectively, and the corresponding estimation errors are \tilde{A} , \tilde{B}_u and \tilde{B}_d . $e_1 = \tilde{A}\tilde{x} + \tilde{B}_u u + \tilde{B}_d d$ is the system identification error. According to the optimal theory [55] and performance index (7), it is known that the value function is

$$V(\tilde{x}(t)) = \int_t^\infty \left(\tilde{x}^T Q \tilde{x} + u^T R u - \gamma^2 \|d\|^2 \right) d\tau. \quad (24)$$

The Hamiltonian for the system (23) can be written as

$$0 = H(\tilde{x}, u^*, d^*, V_{\tilde{x}}^*) = \tilde{x}^T Q \tilde{x} + u^{*T} R u^* - \gamma^2 d^{*T} d^* + V_{\tilde{x}}^{*T} (\hat{A}\tilde{x} + \hat{B}_u u^* + \hat{B}_d d^* + e_1)$$

where

$$u^* = -\frac{1}{2} R^{-1} \hat{B}_u^T V_{\tilde{x}}^*, \quad d^* = \frac{1}{2\gamma^2} \hat{B}_d^T V_{\tilde{x}}^*, \quad V_{\tilde{x}}^* = \frac{\partial V^*}{\partial \tilde{x}}.$$

By using the critic network, the value function can be reconstructed as

$$V^* = W_2^T \psi_2 + e_2 \quad (25)$$

and, its derivative is

$$V_{\tilde{x}}^* = \nabla \psi_2^T W_2 + \nabla e_2$$

where W_2 is the weight of the critic NN. ψ_2 is the activation function of the critic NN, e_2 is the NN reconstruction error, and $\nabla \psi_2$ and ∇e_2 are the derivatives of ψ_2 and e_2 with respect to \tilde{x} , respectively. It is assumed that $\|W_2\| \leq \bar{W}_2$, $\|\psi_2\| \leq \bar{\psi}_2$, $\|\nabla \psi_2\| \leq \bar{\psi}_{d2}$, $\|e_2\| \leq \bar{e}_2$ and $\|\nabla e_2\| \leq \bar{e}_{d2}$ where \bar{W}_2 , $\bar{\psi}_2$, $\bar{\psi}_{d2}$, \bar{e}_2 and \bar{e}_{d2} are positive constants [57]. In the sequel, (25) is approximated by the following critic NN

$$V = \hat{W}_2^T \psi_2 \quad (26)$$

where \hat{W}_2 is the estimation of W_2 . Thus, one can gain

$$V_{\tilde{x}} = \nabla \psi_2^T \hat{W}_2, \quad u = -\frac{1}{2} R^{-1} \hat{B}_u^T \nabla \psi_2^T \hat{W}_2 \quad (27)$$

$$d = \frac{1}{2\gamma^2} \hat{B}_d^T \nabla \psi_2^T \hat{W}_2. \quad (28)$$

Based on (27) and (28), Hamilton-Jacobilsaacs (HJI) can be rewritten as

$$0 = H(\tilde{x}, u, d, V_{\tilde{x}}) = \tilde{x}^T Q \tilde{x} + u^T R u - \gamma^2 d^T d + W_2^T \nabla \psi_2 (\hat{A}\tilde{x} + \hat{B}_u u + \hat{B}_d d) + e_{\text{HJI}}$$

where $e_{\text{HJI}} = (W_2^T \nabla \psi_2 + \nabla e_2) e_1 + \nabla e_2 (\hat{A}\tilde{x} + \hat{B}_u u + \hat{B}_d d)$ is a bounded residual HJI equation error. The above HJI equation can be rewritten as

$$\Theta = -\Xi^T W_2 - e_{\text{HJI}}^T$$

where $\Theta = \tilde{x}^T Q \tilde{x} + u^T R u$, $\Xi = \nabla \psi_2 (\hat{A}\tilde{x} + \hat{B}_u u + \hat{B}_d d)$. Similarly, the auxiliary filters are defined as

$$\begin{aligned} \dot{\mathcal{P}}_2 &= -l_2 \mathcal{P}_2 + \Xi \Xi^T \\ \dot{\mathcal{Q}}_2 &= -l_2 \mathcal{Q}_2 + \Xi \Theta \\ \dot{v}_2 &= -l_2 v_2 + \Xi e_{\text{HJI}}^T \end{aligned}$$

where $\mathcal{P}_2(0) = 0$ and $\mathcal{Q}_2(0) = 0$. l_2 is a positive constant. Thus, we have

$$\mathcal{Q}_2 = -\mathcal{P}_2 W_2 - v_2.$$

Allowing $\tilde{W}_2 = W_2 - \hat{W}_2$, then, the updating law of the critic NN weight \hat{W}_2 is

$$\dot{\hat{W}}_2 = -\Gamma_2 (\mathcal{P}_2 \hat{W}_2 + \mathcal{Q}_2). \quad (29)$$

Lemma 4: Consider critic NN (26) with adaptive law (29). If Ξ is PE, then the critic NN weight error \tilde{W}_2 converges to a compact set around zero for $e_{\text{HJI}} \neq 0$. Moreover, for $e_{\text{HJI}} = 0$, \tilde{W}_2 converges to zero exponentially.

Proof: Similar to the proofs of Theorem 2 in [56] and Theorem 4.1 in [48], thus, the corresponding proof is omitted. ■

Next, the stability of the closed-loop system (6) with (27) and (28) is analysed. By substituting (27) and (28) into (6), one gets

$$\begin{aligned} \dot{\tilde{x}} &= \tilde{A}\tilde{x} + \tilde{B}_u \left(-\frac{1}{2} R^{-1} \tilde{B}_u^T \nabla \psi_2^T \hat{W}_2 + \frac{1}{2} R^{-1} \tilde{B}_u (\nabla \psi_2^T \tilde{W}_2 + \nabla e_2) \right) \\ &\quad + \tilde{B}_d \left(-\frac{1}{2\gamma^2} R^{-1} \tilde{B}_d^T \nabla \psi_2^T \hat{W}_2 - \frac{1}{2\gamma^2} R^{-1} \tilde{B}_d (\nabla \psi_2^T \tilde{W}_2 + \nabla e_2) \right) \\ &\quad + \tilde{B}_u u^{**} + \tilde{B}_d d^{**} \end{aligned} \quad (30)$$

where $\tilde{B}_u = \tilde{B}_u - \hat{B}_u$ and $\tilde{B}_d = \tilde{B}_d - \hat{B}_d$. $u^{**} = -1/2R^{-1}\tilde{B}_u(\nabla\psi_2^T W_2 + \nabla e_2)$, $d^{**} = 1/(2\gamma^2)\tilde{B}_d(\nabla\psi_2^T W_2 + \nabla e_2)$, where u^{**} and d^{**} are the ideal H_∞ control pair to minimize the value function (24). Then, we have the following result.

Lemma 5: Consider the system (6) equipped with (27) and (28) with adaptive laws (22) and (29). If ψ_1 and Ξ are PE, then, the system state \tilde{x} , identifier error \tilde{W}_1 and critic NN weight error \tilde{W}_2 are uniformly ultimately bounded (UUB). Furthermore, u in (27) and d in (28) converge to a bounded set around the ideal H_∞ control solutions u^{**} and d^{**} .

Proof. See Appendix A. ■

Remark 6: From the optimal theory [55], it is known that, for the linear system, the value function and its derivative with respect to \tilde{x} are denoted as $V^* = \frac{1}{2}\tilde{x}^T P^* \tilde{x}$ and $V_{\tilde{x}}^* = P^* \tilde{x}$, respectively. In addition, the value function also can be rewritten as $V^* = \frac{1}{2}(\text{vec}(P^*))^T (\tilde{x} \otimes \tilde{x})$. If the activation function of the critic NN is selected as $\psi_2(\tilde{x}) = \tilde{x} \otimes \tilde{x}$, thus, the corresponding weight is $W_2 = \frac{1}{2}(\text{vec}(P^*))^T$, which implies that $u^* = -R^{-1}\hat{B}_u^T P^* \tilde{x}$, $d^* = \frac{1}{\gamma^2}\hat{B}_d^T P^* \tilde{x}$, and there is no NN reconstruction error, i.e., $e_2 = 0$. So, in this case, according to the proof of Lemma 5, it is shown that, if $e_2 = 0$, the system states can converge to zero and the proposed H_∞ control pair can converge to their ideal solution in ideal case.

Remark 7: Note that if $\Lambda = I$, the system (6) can be reduced to (1), thus, by implementing the above identifier-critic based method, the accurate estimations of the parameters A , B_u , B_d , P_0^* , K_0 and L_0 can be obtained.

From Remarks 6 and 7, it is known that, if the activation function of the critic NN is selected as $\psi_2(\tilde{x}) = \tilde{x} \otimes \tilde{x}$, the unknown parameters in (10) and (11) can converge to the ideal ones. So, one has that the following H_∞ control pairs, which can ensure that the time derivatives of $\mathcal{V}_0 = x^T P_0 x$ and $\mathcal{V}_1 = \tilde{x}^T P_1 \tilde{x}$ are less than 0, respectively,

$$u_0 = -K_0 x, \quad d_0 = L_0 x \quad \text{and} \quad u_1 = -K_1 \tilde{x}, \quad d_1 = L_1 \tilde{x}$$

where $K_0 = R^{-1}\hat{B}_u^T P_0$, $K_1 = R^{-1}\hat{B}_u^T P_1$, and $L_0 = \frac{1}{\gamma^2}\hat{B}_d^T P_0$, $L_1 = \frac{1}{\gamma^2}\hat{B}_d^T P_1$.

Based on the above-obtained available parameters, the method proposed in Section III-A is extended to the data-driven case. Thus, for the system (9) with the unknown parameters, a switched controller is given by

$$u_{\sigma'(t)} = -K_{\sigma'(t)} \tilde{x} \quad (31)$$

$$d_{\sigma'(t)} = L_{\sigma'(t)} \tilde{x} \quad (32)$$

where $\sigma'(t) \in \{0, 1\}$. The available parameters used in the controller are

$$\begin{cases} \hat{A}_0 = \hat{A}, \quad \hat{B}_{u0} = \hat{B}_u, \quad \hat{B}_{d0} = \hat{B}_d \\ \hat{A}_1 = \hat{A}, \quad \hat{B}_{u1} = \hat{B}_u, \quad \hat{B}_{d1} = \hat{B}_d \\ K_0 = R^{-1}\hat{B}_u^T P_0, \quad L_0 = \frac{1}{\gamma^2}\hat{B}_d^T P_0 \\ K_1 = R^{-1}\hat{B}_u^T P_1, \quad L_1 = \frac{1}{\gamma^2}\hat{B}_d^T P_1. \end{cases}$$

A learning-based switching law is given in the following form

$$\sigma'(t) = \begin{cases} i, & V_i(t) \leq \epsilon_i(V_i(t_k')) \\ 1-i, & V_i(t) > \epsilon_i(V_i(t_k')) \end{cases} \quad (33)$$

where $i \in \{0, 1\}$. $\sigma'(t^-) = i$, and $t^- < t$. ϵ_i indicates the observation performance function, and is given in the following form:

$$\epsilon_i(V_i(t_k')) = \eta_0 e^{-a_i(t-t_k')} V_i(t_k') + \eta_\infty$$

where η_0, η_∞ are positive constants satisfying $\eta_0 \geq 1, \eta_\infty \geq 0$. $V_i = \tilde{x}^T P_i \tilde{x}$. $a_i > 0$ satisfies $a_i \leq \alpha_i$ where a_i is a known constant, and $\alpha_i = \lambda_{\max}^{-1}(P_i) \lambda_{\min}(-He(P_i \hat{A}_{1-i} - P_i \hat{B}_{u1} K_i + P_i \hat{B}_{d1} L_i))$ for $i \in \{0, 1\}$. In the sequel, one of the main results can be described in the following theorem.

Theorem 2: Consider system (9), whose system parameters are unknown. Suppose that the system parameter estimations and $P_{\sigma'}$, $\sigma' \in \{0, 1\}$ can be obtained from Lemmas 4 and 5:

1) for no controller-switched case, H_∞ control pair (31) and (32) with the switching law (33) guarantees $\lim_{t \rightarrow \infty} \|\tilde{x}\| \leq \varepsilon$, where $\varepsilon = \eta_\infty \lambda_{\min}^{-\frac{1}{2}}(P_{\sigma'})$;

2) for the controller-switched case, if the following conditions are satisfied

$$\begin{aligned} \alpha_0 \left(1 - \frac{1}{T_1}\right) + \alpha_1 T_2 &> \lambda^*, \quad \lambda^* > \frac{T_\mu}{\tau_D} \\ P_0 &< \mu P_1, \quad P_1 < \mu P_0 \end{aligned} \quad (34)$$

where $T_\mu = 2\ln(\mu) + (\beta_i + \alpha_{1-i})T_{\tau, Mi} + (\beta_{1-i} + \alpha_i)T_{\tau, M(1-i)}$, $\beta_i = \lambda_{\min}^{-1}(P_i) \lambda_{\max}(He(P_i \hat{A}_{1-i} - P_i \hat{B}_{u(1-i)} K_i + P_i \hat{B}_{d(1-i)} L_i))$, thus, H_∞ control pair (31) and (32) with the switching law (33) guarantees that the system (9) is global asymptotically stable.

Proof. The proof is analogous to that of Theorem 1 and omitted. ■

Remark 8: Notice that the existing results on the switched controls against the intermittent attacks mainly include 1) [29] and [34] focus on the intermittent DoS (I-DoS) attack case, and 2) [51] and [52] are concerned with the intermittent actuator failure (I-AF) case. Then, the differences between the existing approached and ours can be described by Table I. Clearly, due to unknown system knowledge and the switching law $\sigma(t)$, under the considered faults, the switched controls in [29], [34], [51] and [52] lose efficacy.

From the above analysis, the proposed reliable control policy can be described in Fig. 4. In Fig. 4, ADP-based learning module indicates the identification-critic based controllers (27), and switched controller represents controller (31) with the switching law (33). The corresponding implementing process can be depicted as follows:

Step 1: Activate the ADP-based learning module. Let $\sigma = 0$. During the learning process, decision module exports u_σ of the ADP-based learning module. It stops until the available parameters $(\hat{A}_\sigma, \hat{B}_{u\sigma}, \hat{B}_{d\sigma}, P_\sigma, u_\sigma, d_\sigma, \sigma)$ are gained, and the obtained available parameters are sent to switched controller.

Step 2: After switched controller receives the available parameters, the decision module exports the control signal u_σ of switched controller. Until the system is abnormal, ADP-based learning module is reactivated. Let $\sigma = 1$, and repeat Step 1.

TABLE I
COMPARISONS OF THE EXISTING SWITCHED CONTROLS AGAINST THE INTERMITTENT ATTACKS

Methods	[29], [34]	[51], [52]	Ours
Attack types	I-DoS	I-AF ($B_d \Delta u$)	I-SDSA ($\bar{x} = \Lambda x$)
Attack parameters	—	$\lambda_i = 0$	$-\infty \leq \lambda_i \leq \infty$
System knowledge	Available	Available	Unavailable
Switching law $\sigma(t)$	Known	Known	Unknown
Switching law $\sigma'(t)$	$\sigma'(t) = \sigma(t)$	$\sigma'(t) = \sigma(t)$	$\sigma'(t) \neq \sigma(t)$

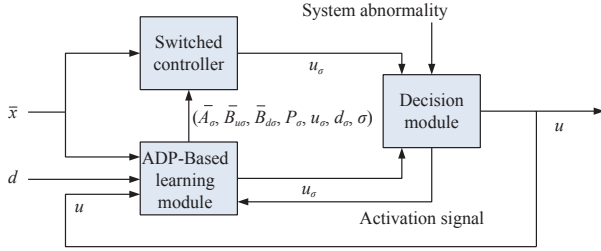


Fig. 4. Diagrammatic sketch of the learning-based switched reliable control policy.

IV. ILLUSTRATIVE EXAMPLE

In this section, the DC motor speed control system is given to validate the presented method, where the control system is shown in Fig. 5. It can be seen that the rotating speed and armature current signals of the motor are transmitted via the network channels 1 and 2, respectively, and the transmission channels are assumed to be vulnerable to cyber attacks. Furthermore, the system parameters are borrowed from [58], where they are obtained from actual measurements and hardware equipments. These parameters are summarized in Table II. Additionally, through the working principle of the DC motor, the dynamics of the motor are represented by

$$\begin{aligned} \dot{I} &= -\left(\frac{R_T}{L_T}\right)I - \left(\frac{C_V}{L_T}\right)\Omega + \left(\frac{1}{L_T}\right)U \\ \dot{\Omega} &= -\left(\frac{1}{J}\right)M_L + \left(\frac{C_T}{J}\right)I \end{aligned}$$

where I is the armature current; Ω is the rotating speed of the motor; and U represents the terminal voltage.

The desired rotating speed and the steady-state current of

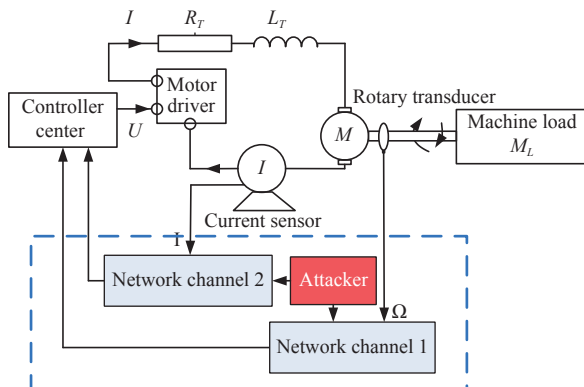


Fig. 5. Block diagram of a DC motor speed control system.

TABLE II
DC MOTOR SPEED CONTROL SYSTEM PARAMETERS

Parameter	Symbol	Value	Unite
Torque constant	C_T	0.06	Nm/A
Machine load	M_L	0.1	Nm
Terminal inductance	L_T	0.3	100H
Terminal resistance	R_T	2.07	Ohm
Rotor inertia	J	80.45×10^{-4}	100 Kg·m ²
Voltage constant	C_V	6.27×10^{-3}	V/rpm

the DC motor are defined as Ω_d and $I_d = M_L/C_T$, respectively. Thus, the tracking errors are $\Delta\Omega = \Omega - \Omega_d$ and $\Delta I = I - I_d$. The dynamics of the errors are given by

$$\begin{bmatrix} \Delta \dot{I} \\ \Delta \dot{\Omega} \end{bmatrix} = \begin{bmatrix} -\frac{R_T}{L_T} & -\frac{C_V}{L_T} \\ \frac{C_T}{J} & 0 \end{bmatrix} \begin{bmatrix} \Delta I \\ \Delta \Omega \end{bmatrix} + \begin{bmatrix} \xi \\ 0 \end{bmatrix} u$$

where $\xi = 2.0039$ and $u = (U - C_V\Omega_d - R_TI_d)/\xi$ is denoted as the control input of the error dynamics. Allowing $x = [\Delta I \ \Delta \Omega]^T$, then the error dynamics can be given in the form of (1) with $B_d = [0.1 \ 0.3]^T$, where the initial system states $x = [1 \ 1]^T$. The disturbance d is considered as a white noise with noise power 0.1.

In order to verify the proposed algorithm, it is assumed that the system parameters are unknown, the control system is equipped with the detector (5) with $\underline{\lambda} = 0.3$ and $\bar{\lambda} = 3$, and the communication channels are subjected to a fault/attack in (2) with $\Lambda = \text{diag}\{-1.5, -0.5\}$, $\eta_f = 0$, $\kappa = 0$, $\tau_D = 75$, $T_1 = 1$ and $T_2 = 0.6$.

Next, the ADP-based learning algorithm in this paper is first implemented to obtain the system parameters for (1) and (6) and the corresponding critic weights. Then we consider the H_∞ performance index (7) with the H_∞ gain $\gamma = 2$, $R = 1$ and $Q = \text{diag}\{1, 1\}$, and the activation function $\psi_2 = [x_1^2 \ x_1x_2 \ x_2^2]^T$ of the critic NN. In the simulation experiment, to accurately estimate the unknown parameters, a probing noise is introduced before 2 s. The initial critic weights are randomly chosen and all the initial values for the parameters in the adaptive laws are set to zero. The ADP-based learning process is shown in Fig. 6. Due to similarity to (1), the learning process for the system (6) is omitted. The obtained optimal estimations of the system parameters and the critic weights are given by

$$\hat{A}_0 = \begin{bmatrix} -6.900 & -0.0209 \\ 7.4580 & 0 \end{bmatrix}, \hat{B}_{u,0} = \begin{bmatrix} 6.6797 \\ 0 \end{bmatrix}, \hat{B}_{d,0} = \begin{bmatrix} 0.1 \\ 0.3 \end{bmatrix}$$

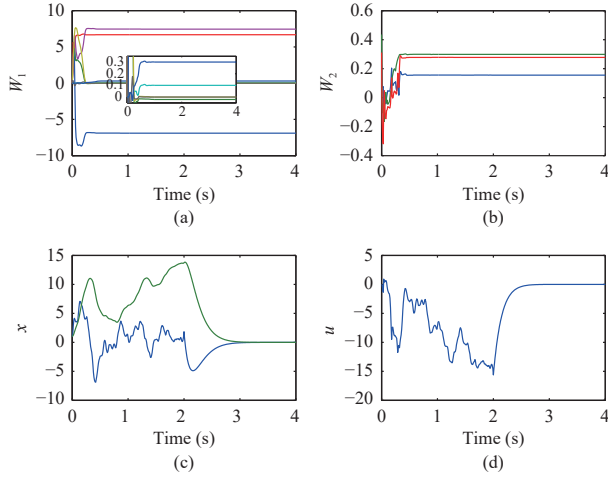


Fig. 6. The ADP-based learning process for the system (1): (a) System parameters; (b) Critic NN weights; (c) System states; (d) Control input signal.

$$\hat{A}_1 = \begin{bmatrix} -6.9000 & -0.0627 \\ 2.4860 & 0 \end{bmatrix}, \hat{B}_{u,1} = \begin{bmatrix} -10.0195 \\ 0 \end{bmatrix}$$

$$\hat{B}_{d,1} = -0.15I_2, W_{2,0} = [0.1557 \quad 0.2988 \quad 0.2776]$$

and

$$W_{2,1} = [0.0713 \quad 0.1986 \quad 0.5630].$$

In the sequel, we test the effectiveness of the reliable switched controller (31) under the intermittent communication faults in the simulation experiment. In the simulation, the disturbance occurs from the initial time to 500 s, and a potential switching signal generated from the fault marker satisfying Assumptions 1 and 2 is considered and plotted by the blue solid line in Fig. 7(a). And then, the parameters of the prescribed performance function used in switching law (33) are chosen as $\eta_0 = 1.1$, $\eta_\infty = 0.05$, $a_0 = 2.6$ and $a_1 = 1.7$. Then, under the communication faults, the switching signal of the controller generated by switching law (33) is denoted by the red dash line in Fig. 7(a). It can be observed that

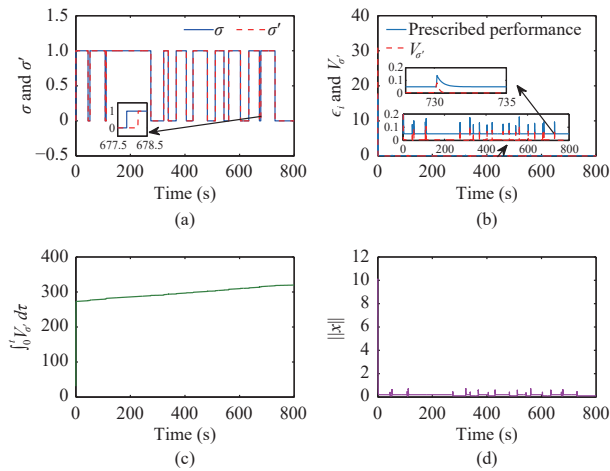


Fig. 7. Simulation results using the proposed method. (a) The system and controller switching signals σ and σ' ; (b) Prescribed performance and system performance $V_{c'}$; (c) The system performance $\int_0^t V_{c'} d\tau$; (d) The norm $\|x\|$ of the system states.

$T_{\tau,M0} \leq 0.353$ and $T_{\tau,M1} \leq 0.353$. Furthermore, by $W_{2,0}$ and $W_{2,1}$, we have $\alpha_0 = 2.6451$, $\alpha_1 = 1.7171$, $\beta_0 = 94.4412$ and $\beta_1 = 109.6481$. We chose $\mu = 5$, thus, by computing, it is obtained that $\lambda^* > T_\mu/\tau_D = 1.0240$, and $\lambda^* < \alpha_0(1 - 1/T_1) + \alpha_1 T_2 = 1.0302$, which implies that condition (34) is satisfied. Under the proposed switching law (33), the system performances are exhibited by Fig. 7(b)–(d). It can be seen that when $V_{c'}$ violates the prescribed performance, the switching of the controllers is triggered, and prior to switching controllers, the performance $V_{c'}$ is inside the prescribed performance. Also, observe that there are some chatters in the trajectory of the norm of the compromised system states. They are caused by passively switching the controllers. These chatters can be improved by reducing the parameters of the prescribed performance. In order to clearly illustrate this, we consider the trajectories of the norm of the compromised system states under four cases: 1) $\eta_\infty = 50$; 2) $\eta_\infty = 5$; 3) $\eta_\infty = 0.5$ and 4) $\eta_\infty = 0.05$. The simulation results are plotted in Fig. 8. It verifies the chatters can be reduced through decreasing η_∞ .

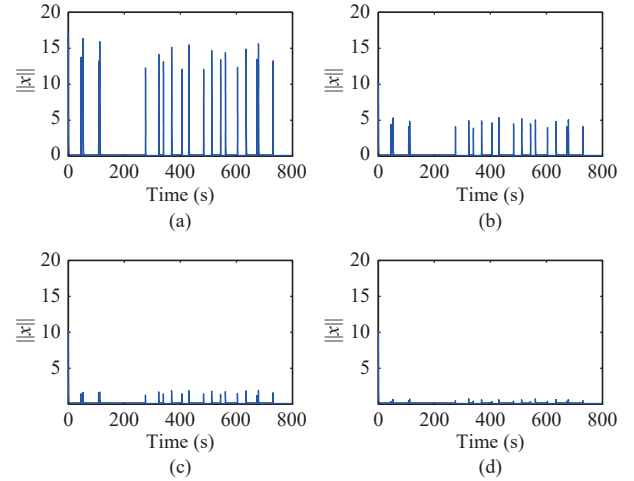


Fig. 8. The norm of the system states under (a) $\eta_\infty = 50$; (b) $\eta_\infty = 5$; (c) $\eta_\infty = 0.5$; (d) $\eta_\infty = 0.05$.

In order to further clarify the advantages of the presented method, a standard ADP-based control (S-ADPC) and an event-triggered ADP-based control (ET-ADPC) [50] schemes are taken into account as comparisons, where ET-ADPC in [50] is one of the latest ADP-based control methods. The control schemes are respectively given as follows:

1) *S-ADPC*: The controller is the form of $u = -\frac{1}{2}R^{-1}\hat{B}_u^T \nabla \psi_2^T \hat{W}_2$, where $R = 1$, $\psi_2 = [x_1^2 \quad x_1 x_2 \quad x_2^2]$ and through the learning algorithm mentioned in Section III-B, the unknown parameters are obtained as $\hat{B}_u = [6.6797 \quad 0]^T$ and $\hat{W}_2 = [0.1557 \quad 0.2988 \quad 0.2776]$.

2) *ET-ADPC* [50]: Select the parameters $Q = \text{diag}\{1, 1\}$ and $R = 1$ in the infinite-horizon integral cost. The controller is form of $u(x_k) = -\frac{1}{2}\hat{B}_u^T \nabla \psi_c(x_k) \hat{W}_c$ with the event-triggered condition $\|e_k\|^2 \leq (1 - t^2)\lambda_{\min}(Q)\|x\|^2/((1 + \mathfrak{I}^2)\mathfrak{I}^2)$ where x_k is the sampled state, $\nabla \psi_c(x_k)$ is the gradient of $\psi_c = [x_{k1}^2 \quad x_{k1}x_{k2} \quad x_{k2}^2]$ with respect to x_k , $e_k = x_k - x(t)$,

$\forall t \in [t_k, t_{k+1})$, and the parameters ι , \mathfrak{I} and \mathcal{J} in the event-triggered condition are chosen as $\iota = 0.2$, $\mathfrak{I} = 1.732$ and $\mathcal{J} = 1.5$. By the algorithm presented in [50], $\tilde{B}_u = [6.6797 \ 0]^T$ and $\tilde{W}_c = [0.1586 \ 0.3034 \ 0.2867]$.

In the following simulation experiment, we consider the same intermittent communication faults as those mentioned above. Then, under S-ADPC and ET-ADPC, the compromised system performances are shown in Fig. 9. It can be seen that the norms $\|x\|$ of the compromised system states under the two control schemes are unstable and the system performances $\int_0^\infty V d\tau$ are degraded severely. Accordingly, through comparisons, the effectiveness of the proposed scheme is verified. In future works, we will further enrich the CPS secure control study for the more general faults/attacks in the packet-dropout and delay environments.

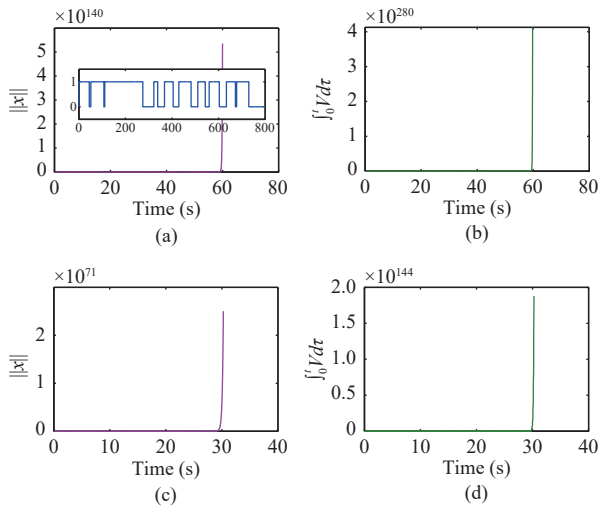


Fig. 9. The system performances: (a) the norm of the system states under S-ADPC; (b) $\int_0^t V d\tau$ under S-ADPC; (c) the norm of the system states under EV-ADPC; and (d) $\int_0^t V d\tau$ under EV-ADPC.

V. CONCLUSION

This paper from the CPS operator's viewpoint studied reliable control problems of data-driven cyber-physical systems with communication faults on multiple channels. Based on our previous result [11], a data-driven switched controller with a prescribed-performance-based switching law was proposed, and through the ADT approach, a fault set, which the closed-loop systems can tolerate, was given. Then, driven by the cooperation of the proposed watermark-based anomaly detector and learning-based switched control policy, the reliability of the systems under the faults was guaranteed. An illustrative example verified the effectiveness of the presented method.

APPENDIX A

THE PROOF OF LEMMA 5

Proof: Consider the following Lyapunov function candidate

$$\mathcal{L}(t) = \mathcal{L}_1(t) + \mathcal{L}_2(t) + \mathcal{L}_3(t) + \mathcal{L}_4(t) \quad (35)$$

where

$$\begin{aligned} \mathcal{L}_1 &= \frac{1}{2} \text{tr}(\tilde{W}_1^T \Gamma_1^{-1} \tilde{W}_1), \quad \mathcal{L}_2 = \frac{1}{2} \text{tr}(\tilde{W}_2^T \Gamma_2^{-1} \tilde{W}_2) \\ \mathcal{L}_3 &= K \tilde{x}^T \tilde{x} + \Gamma V^*, \quad \mathcal{L}_4 = \frac{1}{2} \text{tr}(v_2^T v_2). \end{aligned}$$

From Lemmas 3 and 4, it follows that

$$\dot{\mathcal{L}}_1 \leq -c_1 \|\tilde{W}_1\|^2 \quad (36)$$

$$\dot{\mathcal{L}}_2 \leq -(c_2 - \frac{1}{2\eta}) \|\tilde{W}_2\|^2 + \frac{\eta \|v_2\|^2}{2} \quad (37)$$

where $c_1, c_2 > 0$ are constants. The time derivative of \mathcal{L}_3 is

$$\dot{\mathcal{L}}_3 = 2K \tilde{x} \dot{\tilde{x}} + \Gamma \dot{V}^*. \quad (38)$$

From the value function (24), it is clear that $\dot{V}^* = -(\tilde{x}^T Q \tilde{x} + u^{**T} R u^{**} - \gamma^2 d^{**T} d^{**})$, and then, substituting (30) into (38) yields

$$\begin{aligned} \dot{\mathcal{L}}_3 &= 2K \tilde{x} \left(-\frac{1}{2\gamma^2} \tilde{B}_d (\tilde{B}_d^T \nabla \psi_2^T \tilde{W}_2 + \tilde{B}_d (\nabla \psi_2^T \tilde{W}_2 + \nabla e_2)) \right. \\ &\quad \left. + \tilde{A} \tilde{x} + \frac{1}{2} \tilde{B}_u R^{-1} (\tilde{B}_u^T \nabla \psi_2^T \tilde{W}_2 + \tilde{B}_u (\nabla \psi_2^T \tilde{W}_2 + \nabla e_2)) \right. \\ &\quad \left. + \tilde{B}_u u^{**} + \tilde{B}_d d^{**} \right) - \Gamma (\tilde{x}^T Q \tilde{x} + u^{**T} R u^{**} - \gamma^2 \|d^{**}\|^2). \end{aligned}$$

From $ab \leq \frac{\eta}{2} a^2 + \frac{1}{2\eta} b^2$, $\eta > 0$, we have

$$\begin{aligned} \dot{\mathcal{L}}_3 &\leq \left(-\Gamma \lambda_{\min}(Q) + 2K(\|\tilde{A}\| + 1) \right. \\ &\quad \left. + \frac{1}{2} \eta \lambda_{\max}(R^{-1}) \|\tilde{B}_u\| (\|\tilde{\psi}_{d2}\| \|\hat{W}_2\| + \|\tilde{B}_u\| (\|\tilde{\psi}_{d2}\| + 1)) \right. \\ &\quad \left. + \frac{1}{2\gamma^2} \eta \|\tilde{B}_d\| (\|\tilde{\psi}_{d2}\| \|\hat{W}_2\| + \|\tilde{B}_d\| (\|\tilde{\psi}_{d2}\| + 1)) \right) \|\tilde{x}\|^2 \\ &\quad + \left(K \|\tilde{B}_u\|^2 - \Gamma \lambda_{\min}(R) \right) \|u^{**}\|^2 + \left(K \|\tilde{B}_d\|^2 + \Gamma \gamma^2 \right) \\ &\quad \times \|d^{**}\|^2 + \left(\frac{1}{2\eta} K^2 \lambda_{\max}(R^{-1}) \tilde{\psi}_{d2} \|\tilde{B}_u\| \|\hat{W}_2\| \right. \\ &\quad \left. + \frac{1}{2\eta \gamma^2} \tilde{\psi}_{d2} K^2 \|\tilde{B}_d\| \|\hat{W}_2\| \right) \|\tilde{W}_1\|^2 \\ &\quad + \left(\frac{1}{2\eta} K^2 \lambda_{\max}(R^{-1}) \tilde{\psi}_{d2} \|\tilde{B}_u\|^2 + \frac{1}{2\eta \gamma^2} \tilde{\psi}_{d2} K^2 \|\tilde{B}_d\|^2 \right) \\ &\quad \times \|\tilde{W}_2\|^2 + \left(\frac{1}{2\eta} \lambda_{\max}(R^{-1}) K^2 \|\tilde{B}_u\|^2 + \frac{1}{2\eta \gamma^2} K^2 \|\tilde{B}_d\|^2 \right) \tilde{e}_{d2}^2. \end{aligned} \quad (39)$$

The time derivative of \mathcal{L}_4 is

$$\dot{\mathcal{L}}_4 \leq -(l_2 \Gamma_3 - 4\eta) \|v_2\|^2 + \frac{1}{\eta} \Gamma_3 \|\Xi \varepsilon_{\text{HII}}^T\|^2. \quad (40)$$

Substituting (36), (37), (39) and (40) into (35) yields

$$\begin{aligned} \dot{\mathcal{L}} &\leq -\varepsilon_1 \|v_2\|^2 - \varepsilon_2 \|\tilde{W}_1\|^2 - \varepsilon_3 \|\tilde{W}_2\|^2 \\ &\quad - \varepsilon_4 \|\tilde{x}\|^2 - \varepsilon_5 \|u^*\|^2 + \varepsilon_6 \end{aligned} \quad (41)$$

where

$$\begin{aligned} \varepsilon_1 &= l_2 \Gamma_3 - \frac{9\eta}{2} \\ \varepsilon_2 &= c_1 - \frac{1}{2\eta} K^2 \lambda_{\max}(R^{-1}) \tilde{\psi}_{d2} \|\tilde{B}_u\| \|\hat{W}_2\| \\ &\quad - \frac{1}{2\eta \gamma^2} \tilde{\psi}_{d2} K^2 \|\tilde{B}_d\| \|\hat{W}_2\| \end{aligned}$$

$$\begin{aligned}
\varepsilon_3 &= c_2 - \frac{1}{2\eta} - \frac{1}{2\eta} K^2 \lambda_{\max}(R^{-1}) \bar{\psi}_{d2} \|\tilde{B}_u\|^2 \\
&\quad - \frac{1}{2\eta\gamma^2} \bar{\psi}_{d2} K^2 \|\tilde{B}_u\|^2 \\
\varepsilon_4 &= \Gamma \lambda_{\min}(Q) - 2K(\|\tilde{A}\| + 1) \\
&\quad - \frac{1}{2} \eta \lambda_{\max}(R^{-1}) \|\tilde{B}_u\|(\bar{\psi}_{d2} \|\hat{W}_2\| \\
&\quad + \|\tilde{B}_u\|(\bar{\psi}_{d2} + 1)) - \frac{1}{2\gamma^2} \eta \|\tilde{B}_d\|(\bar{\psi}_{d2} \|\hat{W}_2\| \\
&\quad + \|\tilde{B}_d\|(\bar{\psi}_{d2} + 1)) \\
\varepsilon_5 &= -K\|\tilde{B}_u\|^2 + \Gamma \lambda_{\min}(R) \\
\varepsilon_6 &= \left(K\|\tilde{B}_d\|^2 + \Gamma\gamma^2\right) \|\bar{d}^{**}\|^2 + \frac{1}{\eta} \Gamma_3 \|\Xi \varepsilon_{\text{HJI}}^T\|^2 \\
&\quad + \left(\frac{1}{2\eta} \lambda_{\max}(R^{-1}) K^2 \|\tilde{B}_u\|^2 + \frac{1}{2\eta\gamma^2} K^2 \|\tilde{B}_d\|^2\right) \bar{e}_{d2}^2.
\end{aligned}$$

Hence, if the designed parameters Γ , K and η satisfies the following conditions

$$\varepsilon_1 > 0, \quad \varepsilon_2 > 0, \quad \varepsilon_3 > 0, \quad \varepsilon_4 > 0, \quad \varepsilon_5 > 0$$

thus, from (41), it is deduced that \tilde{x} , \tilde{W}_1 , \tilde{W}_2 and v_2 are UUB.

Next, the errors between (27), (28) and the ideal ones are analysed. The corresponding errors are

$$\begin{aligned}
u - u^{**} &= -\frac{1}{2} R^{-1} \hat{B}_u^T \nabla \psi_2^T \hat{W}_2 + \frac{1}{2} R^{-1} \tilde{B}_u^T (\nabla \psi_2^T W_2 + \nabla e_2) \\
&= \frac{1}{2} R^{-1} \tilde{B}_u^T \nabla \psi_2^T \hat{W}_2 + \frac{1}{2} R^{-1} \tilde{B}_u^T \nabla e_2 \\
&\quad + \frac{1}{2} R^{-1} \tilde{B}_u^T \nabla \psi_2^T W_2 - \frac{1}{2} R^{-1} \tilde{B}_u^T \nabla \psi_2^T \tilde{W}_2 \\
d - d^{**} &= \frac{1}{2\gamma^2} \hat{B}_d^T \nabla \psi_2^T \hat{W}_2 - \frac{1}{2\gamma^2} \tilde{B}_d^T (\nabla \psi_2^T W_2 + \nabla e_2) \\
&= \frac{1}{2\gamma^2} \tilde{B}_d^T \nabla \psi_2^T \hat{W}_2 - \frac{1}{2\gamma^2} \tilde{B}_d^T \nabla \psi_2^T W_2 \\
&\quad + \frac{1}{2\gamma^2} \tilde{B}_d^T \nabla \psi_2^T \tilde{W}_2 - \frac{1}{2\gamma^2} \tilde{B}_d^T \nabla e_2.
\end{aligned}$$

According to the above analysis, one has

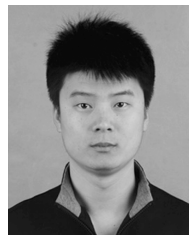
$$\begin{aligned}
\lim_{t \rightarrow \infty} \|u - u^{**}\| &\leq \frac{1}{2} \lambda_{\min}(R) (\|\tilde{B}_u\| \|\nabla \psi_2\| \|\tilde{W}_2\| \\
&\quad + \|\tilde{B}_u\| \|\nabla e_2\| + \|\tilde{W}_1\| \|\nabla \psi_2\| \|W_2\| \\
&\quad + \|\tilde{W}_1\| \|\nabla \psi_2\| \|\tilde{W}_2\|) \leq e_u \\
\lim_{t \rightarrow \infty} \|d - d^{**}\| &\leq \frac{1}{2\gamma^2} (\|\tilde{B}_d\| \|\nabla \psi_2\| \|\tilde{W}_2\| \\
&\quad + \|\tilde{W}_1\| \|\nabla \psi_2\| \|W_2\| + \|\tilde{W}_1\| \|\nabla \psi_2\| \|\tilde{W}_2\| \\
&\quad + \|\tilde{B}_d\| \|\nabla e_2\|) \leq e_d
\end{aligned}$$

where e_u and e_d are positive constants, which are determined by the NN approximation errors. ■

REFERENCES

- [1] J. L. Liu, Z. G. Wu, D. Yue, and J. H. Park, "Stabilization of networked control systems with hybrid-driven mechanism and probabilistic cyber attacks," *IEEE Trans. Syst., Man, Cybern.: Syst.*, DOI: 10.1109/tsmc.2018.2888633, Jan. 2019.
- [2] T. Liu, B. Tian, Y. F. Ai, and F.-Y. Wang, "Parallel reinforcement learning-based energy efficiency improvement for a cyber-physical system," *IEEE/CAA J. Autom. Sinica*, vol. 7, no. 2, pp. 617–626, Mar. 2020.
- [3] D. R. Ding, Q. L. Han, Y. Xiang, X. H. Ge, and X. M. Zhang, "A survey on security control and attack detection for industrial cyber-physical systems," *Neurocomputing*, vol. 275, pp. 1674–1683, Jan. 2018.
- [4] J. L. Liu, L. L. Wei, X. P. Xie, E. G. Tian, and S. M. Fei, "Quantized stabilization for T-S fuzzy systems with hybrid-triggered mechanism and stochastic cyber-attacks," *IEEE Trans. Fuzzy Syst.*, vol. 26, no. 6, pp. 3820–3834, Dec. 2018.
- [5] W. Sun, S. F. Su, J. W. Xia, and V. T. Nguyen, "Adaptive fuzzy tracking control of flexible-joint robots with full-state constraints," *IEEE Trans. Syst., Man, Cybern.: Syst.*, vol. 49, no. 11, pp. 2201–2209, Nov. 2019.
- [6] J. B. Qiu, H. J. Gao, and S. X. Ding, "Recent advances on fuzzy-model-based nonlinear networked control systems: a survey," *IEEE Trans. Ind. Electron.*, vol. 63, no. 2, pp. 1207–1217, Feb. 2016.
- [7] X. Z. Jin, G. H. Yang, and L. Peng, "Robust adaptive tracking control of distributed delay systems with actuator and communication failures," *Asian J. Control*, vol. 14, no. 5, pp. 1282–1298, Sep. 2012.
- [8] M. Al Janaideh, E. Hammad, A. Farraj, and D. Kundur, "Mitigating attacks with nonlinear dynamics on actuators in cyber-physical mechatronic systems," *IEEE Trans. Ind. Inform.*, vol. 15, no. 9, pp. 4845–4856, Sep. 2019.
- [9] W. Sun, S. F. Su, Y. Q. Wu, J. W. Xia, and V. T. Nguyen, "Adaptive fuzzy control with high-order barrier Lyapunov functions for high-order uncertain nonlinear systems with full-state constraints," *IEEE Trans. Cybern.*, DOI: 10.1109/tycyb.2018.2890256, Jan. 2019.
- [10] M. S. Mahmoud, M. M. Hamdan, and U. A. Baroudi, "Modeling and control of cyber-physical systems subject to cyber attacks: a survey of recent advances and challenges," *Neurocomputing*, vol. 338, pp. 101–115, Nov. 2019.
- [11] X. Huang and J. X. Dong, "On modeling and secure control of cyber-physical systems with attacks/faults changing system dynamics: an average dwell-time approach," *Int. J. Robust Nonlinear Control*, vol. 29, no. 16, pp. 5481–5498, Nov. 2019.
- [12] H. Zhang, P. Cheng, L. Shi, and J. M. Chen, "Optimal denial-of-service attack scheduling with energy constraint," *IEEE Trans. Autom. Control*, vol. 60, no. 11, pp. 3023–3028, Nov. 2015.
- [13] Y. Tang, D. D. Zhang, D. W. C. Ho, W. Yang, and B. Wang, "Event-based tracking control of mobile robot with denial-of-service attacks," *IEEE Trans. Syst., Man, Cybern.: Syst.*, DOI: 10.1109/tsmc.2018.2875793, Nov. 2018.
- [14] Y. Liu, P. Ning, and M. K. Reiter, "False data injection attacks against state estimation in electric power grids," *ACM Trans. Inf. Syst. Secur.*, vol. 14, no. 1, pp. 13, Jun. 2011.
- [15] G. Y. Wu, J. Sun, and J. Chen, "Optimal data injection attacks in cyber-physical systems," *IEEE Trans. Cybern.*, vol. 48, no. 12, pp. 3302–3312, Dec. 2018.
- [16] Y. L. Mo, S. Weerakkody, and B. Sinopoli, "Physical authentication of control systems: Designing watermarked control inputs to detect counterfeit sensor outputs," *IEEE Control Syst.*, vol. 35, no. 1, pp. 93–109, Feb. 2015.
- [17] A. Hoehn and P. Zhang, "Detection of replay attacks in cyber-physical systems," in *Proc. American Control Conf. (ACC)*, Boston, USA, 2016, pp. 290–295.
- [18] X. Jin, W. M. Haddad, and T. Yucelen, "An adaptive control architecture for mitigating sensor and actuator attacks in cyber-physical systems," *IEEE Trans. Autom. Control*, vol. 62, no. 11, pp. 6058–6064, Nov. 2017.
- [19] Z. Y. Guo, D. W. Shi, K. H. Johansson, and L. Shi, "Optimal linear cyber-attack on remote state estimation," *IEEE Trans. Control Network Syst.*, vol. 4, no. 1, pp. 4–13, Mar. 2017.
- [20] X. J. Li and X. Y. Shen, "A data-driven attack detection approach for DC servo motor systems based on mixed optimization strategy," *IEEE Trans. Ind. Inform.*, DOI: 10.1109/tii.2019.2960616, Dec. 2019.
- [21] F. Pasqualetti, F. Dörfler, and F. Bullo, "Attack detection and identification in cyber-physical systems," *IEEE Trans. Autom. Control*, vol. 58, no. 11, pp. 2715–2729, Nov. 2013.
- [22] K. G. Vamvoudakis, J. P. Hespanha, B. Sinopoli, and Y. L. Mo, "Detection in adversarial environments," *IEEE Trans. Autom. Control*, vol. 59, no. 12, pp. 3209–3223, Dec. 2014.
- [23] H. Fawzi, P. Tabuada, and S. Diggavi, "Secure estimation and control

- for cyber-physical systems under adversarial attacks,” *IEEE Trans. Autom. Control*, vol. 59, no. 6, pp. 1454–1467, Jun. 2014.
- [24] A. Teixeira, I. Shames, H. Sandberg, and K. H. Johansson, “A secure control framework for resource-limited adversaries,” *Automatica*, vol. 51, pp. 135–148, Jan. 2015.
- [25] Y. Chen, S. Kar, and J. M. F. Moura, “Dynamic attack detection in cyber-physical systems with side initial state information,” *IEEE Trans. Autom. Control*, vol. 62, no. 9, pp. 4618–4624, Sep. 2017.
- [26] J. X. Dong, Y. Wu, and G. H. Yang, “A new sensor fault isolation method for T-S fuzzy systems,” *IEEE Trans. Cybern.*, vol. 47, no. 9, pp. 2437–2447, Sep. 2017.
- [27] W. Ao, Y. D. Song, and C. Y. Wen, “Adaptive cyber-physical system attack detection and reconstruction with application to power systems,” *IET Control Theory Appl.*, vol. 10, no. 12, pp. 1458–1468, Aug. 2016.
- [28] J. Yang, C. J. Zhou, S. H. Yang, H. Z. Xu, and B. W. Hu, “Anomaly detection based on zone partition for security protection of industrial cyber-physical systems,” *IEEE Trans. Ind. Electron.*, vol. 65, no. 5, pp. 4257–4267, May 2018.
- [29] M. S. Mahmoud and Y. Q. Xia, *Networked Control Systems: Cloud Control and Secure Control*. Kidlington, UK: Butterworth-Heinemann, 2019.
- [30] H. H. Yuan, Y. Q. Xia, J. H. Zhang, H. J. Yang, and M. S. Mahmoud, “Stackelberg-game-based defense analysis against advanced persistent threats on cloud control system,” *IEEE Trans. Ind. Inform.*, vol. 16, no. 3, pp. 1571–1580, Mar. 2020.
- [31] A. Kanellopoulos and K. G. Vamvoudakis, “A moving target defense control framework for cyber-physical systems,” *IEEE Trans. Autom. Control*, vol. 65, no. 3, pp. 1029–1043, Mar. 2020.
- [32] A. Y. Lu and G. H. Yang, “Event-triggered secure observer-based control for cyber-physical systems under adversarial attacks,” *Inform. Sci.*, vol. 420, pp. 96–109, Dec. 2017.
- [33] X. Huang and J. X. Dong, “Reliable control policy of cyber-physical systems against a class of frequency-constrained sensor and actuator attacks,” *IEEE Trans. Cybern.*, vol. 48, no. 12, pp. 3432–3439, Dec. 2018.
- [34] C. De Persis and P. Tesi, “Input-to-state stabilizing control under denial-of-service,” *IEEE Trans. Autom. Control*, vol. 60, no. 11, pp. 2930–2944, Nov. 2015.
- [35] S. Feng and P. Tesi, “Resilient control under denial-of-service: robust design,” *Automatica*, vol. 79, pp. 42–51, May 2017.
- [36] T. Yucelen, W. M. Haddad, and E. M. Feron, “Adaptive control architectures for mitigating sensor attacks in cyber-physical systems,” *Cyber-Phys. Syst.*, vol. 2, no. 1–4, pp. 24–52, Oct. 2016.
- [37] L. W. An and G. H. Yang, “Improved adaptive resilient control against sensor and actuator attacks,” *Inform. Sci.*, vol. 423, pp. 145–156, Jan. 2018.
- [38] X. Huang, D. Zhai, and J. X. Dong, “Adaptive integral sliding-mode control strategy of data-driven cyber-physical systems against a class of actuator attacks,” *IET Control Theory Appl.*, vol. 12, no. 10, pp. 1440–1447, Jul. 2018.
- [39] S. Yin, H. J. Gao, S. Ding, and Z. Wang, “Data-based control and process monitoring with industrial applications,” *IET Control Theory Appl.*, vol. 9, no. 7, pp. 997–999, Apr. 2015.
- [40] Y. Jiang and Z. P. Jiang, “Computational adaptive optimal control for continuous-time linear systems with completely unknown dynamics,” *Automatica*, vol. 48, no. 10, pp. 2699–2704, Oct. 2012.
- [41] H. Modares, F. L. Lewis, and M. B. Naghibi-Sistani, “Adaptive optimal control of unknown constrained-input systems using policy iteration and neural networks,” *IEEE Trans. Neural Networks Learn. Syst.*, vol. 24, no. 10, pp. 1513–1525, Oct. 2013.
- [42] M. Wang and A. L. Yang, “Dynamic learning from adaptive neural control of robot manipulators with prescribed performance,” *IEEE Trans. Syst., Man, Cybern.: Syst.*, vol. 47, no. 8, pp. 2244–2255, Aug. 2017.
- [43] Y. Yuan, H. H. Yuan, Z. D. Wang, L. Guo, and H. J. Yang, “Optimal control for networked control systems with disturbances: a delta operator approach,” *IET Control Theory Appl.*, vol. 11, no. 9, pp. 1325–1332, Jun. 2017.
- [44] Y. Yuan, L. Guo, and Z. D. Wang, “Composite control of linear quadratic games in delta domain with disturbance observers,” *J. Franklin Inst.*, vol. 354, no. 4, pp. 1673–1695, Mar. 2017.
- [45] Q. L. Wei, R. Z. Song, and P. F. Yan, “Data-driven zero-sum neuro-optimal control for a class of continuous-time unknown nonlinear systems with disturbance using ADP,” *IEEE Trans. Neural Networks Learn. Syst.*, vol. 27, no. 2, pp. 444–458, Feb. 2016.
- [46] H. L. Li, D. R. Liu, and D. Wang, “Integral reinforcement learning for linear continuous-time zero-sum games with completely unknown dynamics,” *IEEE Trans. Autom. Sci. Eng.*, vol. 11, no. 3, pp. 706–714, Jul. 2014.
- [47] B. Luo, D. R. Liu, H. N. Wu, D. Wang, and F. L. Lewis, “Policy gradient adaptive dynamic programming for data-based optimal control,” *IEEE Trans. Cybern.*, vol. 47, no. 10, pp. 3341–3354, Oct. 2017.
- [48] Y. F. Lv, J. Na, and X. M. Ren, “Online H_∞ control for completely unknown nonlinear systems via an identifier-critic-based ADP structure,” *Int. J. Control*, vol. 92, no. 1, pp. 100–111, 2019.
- [49] K. G. Vamvoudakis and H. Ferraz, “Model-free event-triggered control algorithm for continuous-time linear systems with optimal performance,” *Automatica*, vol. 87, pp. 412–420, Jan. 2018.
- [50] X. Yang and H. B. He, “Adaptive critic designs for event-triggered robust control of nonlinear systems with unknown dynamics,” *IEEE Trans. Cybern.*, vol. 49, no. 6, pp. 2255–2267, Jun. 2019.
- [51] C. Y. Wu, C. S. Li, and J. Zhao, “Switching-based state tracking of model reference adaptive control systems in the presence of intermittent failures of all actuators,” *Int. J. Adapt. Control Signal Process.*, vol. 28, no. 11, pp. 1094–1105, Nov. 2014.
- [52] R. Wang, J. Zhao, G. M. Dimirovski, and G. P. Liu, “Output feedback control for uncertain linear systems with faulty actuators based on a switching method,” *Int. J. Robust Nonlinear Control*, vol. 19, no. 12, pp. 1295–1312, Aug. 2009.
- [53] A. Gelb and W. E. Velde, *Multiple-Input Describing Functions and Nonlinear System Design*. New York: McGraw-Hill, 1968.
- [54] W. J. Rugh, *Linear System Theory*. 2nd ed. Upper Saddle River, USA: Prentice Hall, 1996.
- [55] F. L. Lewis, D. L. Vrabie, and V. L. Syrmos, *Optimal Control*. New York, USA: John Wiley & Sons, 2012.
- [56] J. Na, J. Yang, X. Wu, and Y. Guo, “Robust adaptive parameter estimation of sinusoidal signals,” *Automatica*, vol. 53, pp. 376–384, Mar. 2015.
- [57] M. Abu-Khalaf and F. L. Lewis, “Nearly optimal control laws for nonlinear systems with saturating actuators using a neural network HJB approach,” *Automatica*, vol. 41, no. 5, pp. 779–791, May 2005.
- [58] J. S. Wang and G. H. Yang, “Output-feedback control of unknown linear discrete-time systems with stochastic measurement and process noise via approximate dynamic programming,” *IEEE Trans. Cybern.*, vol. 48, no. 7, pp. 1977–1988, Jul. 2018.



Xin Huang is currently pursuing the Ph.D. degree in navigation, guidance and control from Northeastern University. His research interests include cyber-physical system security, reliable control, and adaptive control.

Mr. Huang was a recipient of the Excellent Master Dissertation Award of Shanxi Province in 2016.



Jiuxiang Dong (M'12) received the B.S. degree in mathematics and applied mathematics, the M.S. degree in applied mathematics from Liaoning Normal University, in 2001 and 2004, respectively. He received the Ph.D. degree in navigation guidance and control from Northeastern University, in 2009. He is currently a Professor at the College of Information Science and Engineering, Northeastern University. His research interests include fuzzy control, robust control, and reliable control.

Dr. Dong is an Associate Editor for the *International Journal of Control, Automation, and Systems (IJCAS)*.